

Self-consistent numerical-basis-set linear-combination-of-atomic-orbitals model for the study of solids in the local density formalism

Alex Zunger and A. J. Freeman

Physics Department and Materials Research Center, Northwestern University, Evanston, Illinois 60201

(Received 26 July 1976)

A new approach to the fully self-consistent solution of the one-particle equations in a periodic solid within the Hohenberg-Kohn-Sham local-density-functional formalism is presented. The method is based on systematic extensions of non-self-consistent real-space techniques of Ellis, Painter, and collaborators and the self-consistent reciprocal-space methodologies of Chaney, Lin, Lafon, and co-workers. Specifically, our approach combines a discrete variational treatment of all potential terms (Coulomb, exchange, and correlation) arising from the superposition of spherical atomlike overlapping charge densities, with a rapidly convergent three-dimensional Fourier series representation of all the multicenter potential terms that are not expressible by a superposition model. The basis set consists of the exact numerical valence orbitals obtained from a direct solution of the local-density atomic one-particle equations and (for increased variational freedom) virtual numerical atomic orbitals, charge-transfer (ion-pair) orbitals, and "free" Slater one-site functions. The initial crystal potential consists of a non-muffin-tin superposition potential, including nongradient free-electron correlation terms calculated beyond the random-phase approximation. The usual multicenter integrations encountered in the linear-combination-of-atomic-orbitals tight-binding formalism are avoided by calculating all the Hamiltonian and other matrix elements between Bloch states by three-dimensional numerical Diophantine integration. In the first stage of self-consistency, the atomic superposition potential and the corresponding numerical basis orbitals are modified simultaneously and *nonlinearly* by varying (iteratively) the atomic occupation numbers (on the basis of computed Brillouin-zone averaged band populations) so as to minimize the deviation, $\Delta\rho(\vec{r})$, between the band charge density and the superposition charge density. This step produces the "best" atomic configuration within the superposition model for the crystal charge density and tends to remove all the sharp "localized" features in the function $\Delta\rho(\vec{r})$ by allowing for intra-atomic charge redistribution to take place. In the second stage, the three-dimensional multicenter Poisson equation associated with $\Delta\rho(\vec{r})$ through a Fourier series representation of $\Delta\rho(\vec{r})$ is solved and solutions of the band problem are found using a self-consistent criterion on the Fourier coefficients of $\Delta\rho(\vec{r})$. The calculated observables include the total crystal ground-state energy, equilibrium lattice constants, electronic pressure, x-ray scattering factors, and directional Compton profile. The efficiency and reliability of the method is illustrated by means of results obtained for some ground-state properties of diamond; comparisons are made with the predictions of other methods.

I. INTRODUCTION

The current popularity of energy-band theory stems from its successful application to the study of increasingly diverse problems in solid-state physics. Recent new sophisticated experiments on both traditional materials and those having complex crystallographic structures have demanded, however, not only theoretical descriptions of phenomena related to the one-electron *eigenvalue* but also detailed and precise *wave functions* with which to determine the expectation values of different observable operators. Such a demanding test of the predictions of one-electron theory has the additional virtue in permitting, by their comparison with experiment, accurate determinations of the relative magnitude and importance of many-body effects in real solids. Thus, there has developed considerable interest in applying the Hohenberg-Kohn-Sham^{1,2} local-density-functional (LDF) formalism to the investigation of various ground-state properties of solids, despite the usual difficulties of solving the associated one-

particle equation characterized by a multicenter nonspherical potential. A variety of well-known approximations have been introduced in order to reduce the complexity of the problem. For example, the various forms of orthogonalized-plane-wave (OPW) techniques^{3,4} suffer from serious convergence difficulties when applied to solids containing first-row atoms with no *p* states in the atomic cores. Recent studies with extended sets of orthogonalized plane waves⁵ have indicated errors in the eigenvalues of the order of up to a few volts due to poor convergence in calculations employing several hundreds of OPW's. The muffin-tin approximations applied to augmented-plane-wave (APW) calculations^{6,7} have been recently criticized as introducing errors of up to a rydberg in the potential in diamond⁸ and other covalent structures,⁹ and overestimating the binding energy in some covalently bonded molecules by as much as (100–300)%.¹⁰ Recent LCAO (linear orbitals)-type calculations^{11–13} have overcome the difficulty of treating non-muffin-tin potentials and have demonstrated that efficient convergence with respect

to the size of the basis set¹³ can be obtained. However, the problem of carrying this type of calculation towards self-consistency still remains a formidable task within the framework of present techniques. It thus seems that although it is possible to obtain reasonable results for the eigenvalues of the local-density one-particle equations within the above-mentioned approximations both for some molecules^{14, 15} and solids (i.e., band structures), and accurate evaluation of the predictions of this theory for ground-state functionals of the electron density is still a nontrivial task for state-of-the-art methods in one-electron theory.

In this paper, we describe a new approach to the fully self-consistent (SC) solutions of the one-particle equations in a periodic solid within the local-density-functional formalism. It is designed and developed to incorporate special features with which to overcome difficulties encountered by other methods. Specifically, as will be shown in detail, the method combines a discrete variational treatment of all potential terms (Coulomb, exchange, and correlation) arising from the superposition of spherical atomiclike overlapping charge densities, with a rapidly convergent three-dimensional Fourier-series representation of all the multicenter potential terms that are not expressible by a superposition model. The basis set consists of the accurate numerical valence orbitals obtained from a direct solution of the local-density *atomic* one-particle equations. To obtain increased variational freedom, this basis set is then augmented by virtual (numerical) atomic orbitals, charge-transfer (ion pair) orbitals, and "free" Slater one-site functions. The initial crystal potential consists of a non-muffin-tin superposition potential, including nongradient free-electron correlation terms calculated beyond the random-phase approximation. The Hamiltonian matrix elements between Bloch states are calculated by the three-dimensional Diophantine integration scheme of Haselgrove,¹⁶ and Ellis and Painter,¹⁷ thereby avoiding the usual multicenter integrations encountered in the LCAO tight-binding formalism. Self-consistency is obtained in two stages: in the first state ("charge and configuration self-consistency"), the atomic superposition potential and the corresponding numerical basis orbitals are modified simultaneously and *non-linearly* by varying (iteratively) the atomic occupation numbers (on the basis of the computed Brillouin-zone averaged band population) so as to minimize the deviation $\Delta\rho(\vec{r})$ between the band charge density and the superposition charge density. This step produces the "best" atomic configuration (for the employed numerical basis

orbitals) within the superposition model for the crystal charge density and tends to remove all the sharp "localized" features in the function $\Delta\rho(\vec{r})$ by allowing for intra-atomic charge redistribution to take place. Having obtained a low-amplitude smooth function $\Delta\rho(\vec{r})$ that contains zero charge, we proceed in the second state of self-consistency to solve the three-dimensional multicenter Poisson equation associated with $\Delta\rho(\vec{r})$ through a Fourier-series representation of $\Delta\rho(\vec{r})$. The solution of the band problem is repeated until the changes in the Fourier coefficients of $\Delta\rho(\vec{r})$ in successive iterations are lower than a prescribed tolerance. The calculated quantities include the total crystal ground-state energy, equilibrium lattice constants, electronic pressure, x-ray scattering factors, and directional Compton profile in addition to the one-electron band structure.

Section II reviews those elements of the local-density-functional formalism which are the basis of this work. Section III describes some basic elements (crystal potential, basis functions, and Hamiltonian matrix elements) needed to obtain fully self-consistent solutions by the method discussed in Sec. IV. Of particular concern to us is the question of the role of the usual approximations used to solve the LDF problem—muffin-tin potential,¹⁸⁻²⁰ non-self-consistency¹⁸ on the ground-state properties of solids. In Sec. V, we present illustrative results of energy-band studies of diamond which are compared with the predictions of other theoretical calculations.

II. LOCAL-DENSITY-FUNCTIONAL FORMALISM

The Hohenberg-Kohn-Sham^{1, 2} local-density formalism is based on the fundamental theorem that the ground-state properties of an inhomogeneous interacting electron system are functionals of the electron density $\rho(\vec{r})$ and that in the presence of an external potential $V_{\text{ext}}(\vec{r})$ the total ground-state energy in its lowest variational state can be written

$$E(\rho(\vec{r})) = \int V_{\text{ext}}(\vec{r})\rho(\vec{r}) d\vec{r} + G(\rho(\vec{r})), \quad (1)$$

where $G(\rho(\vec{r}))$ is a universal functional of $\rho(\vec{r})$ and is *independent of the external potential* $V_{\text{ext}}(\vec{r})$. This theorem forms the basis of our approach to the electronic structure problem in that it provides an effective one-particle equation relating self-consistently the ground-state wave functions to the energy functionals (i.e., potential) of the electronic system. Identifying the external potential for a polyatomic system as the electron-nuclear and internuclear interactions and varying $E(\rho(\vec{r}))$ with respect to $\rho(\vec{r})$, one obtains an effective one-particle equation of the form

$$\left(-\frac{1}{2}\nabla^2 - \sum_m \frac{Z_m}{|\vec{R}_m - \vec{r}|} + \int \frac{\rho(\vec{r}')}{|\vec{r} - \vec{r}'|} d\vec{r}' + \frac{\delta E_{xc}(\rho(\vec{r}))}{\delta \rho(\vec{r})}\right) \psi_j(\vec{r}) = \epsilon_j \psi_j(\vec{r}), \quad (2)$$

where the exact quantum-mechanical Laplacian operator replaces the noninteracting kinetic energy. Here Z_m denotes the nuclear charge of the particle at site \vec{R}_m and $E_{xc}(\rho(\vec{r}))$ the total exchange and correlation energy of the interacting (inhomogeneous) electron system (bold-face parentheses are used to denote functional dependence). The eigenfunctions $\psi_j(\vec{r})$ are simply related to the total ground-state charge density of the σ_{oc} occupied one-particle states by

$$\rho(\vec{r}) = \sum_{j=1}^{\sigma_{oc}} \psi_j^*(\vec{r}) \psi_j(\vec{r}), \quad (3)$$

which, in turn, determines self-consistently the local-density functional in Eq. (2). The total ground-state energy is then given by

$$E_{tot} = \sum_{j=1}^{\sigma_{oc}} \langle \psi_j(\vec{r}) | -\frac{1}{2}\nabla^2 | \psi_j(\vec{r}) \rangle + \int \rho(\vec{r}) \left(\sum_m \frac{Z_m}{|\vec{r} - \vec{R}_m|} + \frac{1}{2} \int \frac{\rho(\vec{r}')}{|\vec{r} - \vec{r}'|} d\vec{r}' \right) d\vec{r} \\ + \sum_{\substack{n, m \\ n \neq m}} \frac{Z_n Z_m}{|\vec{R}_n - \vec{R}_m|} + E_{xc}(\rho(\vec{r})), \quad (4)$$

where the first term represents the kinetic energy, the second and third terms are the total electrostatic potential energy, and the last term is the exchange and correlation energy.

No satisfactory formulation of $E_{xc}(\rho(\vec{r}))$ has been obtained so far for a general $\rho(\vec{r})$. In the limit of slowly varying density, gradient expansions of $E_{xc}(\rho(\vec{r}))$ have been suggested.^{2,21} Although there seem to be no compelling evidence for the possible suitability of such expansions to realistic models of polyatomic systems (nor is there any convincing argument as to the convergence rate of this expansion), there still seems to be some interest in applying the LDF formalism with the presently available first-term expansion of $E_{xc}(\rho(\vec{r}))$ as a first step towards a more complete electronic structure theory based on accurate local-density functionals. Note that the LDF formalism in the form described above makes no claim on the physical significance of the eigenvalues ϵ_j in Eq. (2); hence we concentrate only on ground-state crystal properties.

Retaining only the nongradient terms in the expansion of $E_{xc}(\rho(\vec{r}))$, the exchange and correlation potential becomes

$$\delta E_{xc}(\rho(\vec{r}))/\delta \rho(\vec{r}) \cong F_{ex}(\rho(\vec{r})) + F_{corr}(\rho(\vec{r})), \quad (5)$$

where the exchange potential has the well-known form

$$F_{ex}(\rho(\vec{r})) = \frac{4}{3} \epsilon_x(\rho(\vec{r})) \cong -[(3/\pi)\rho(\vec{r})]^{1/3}, \quad (6)$$

where $\epsilon_x(\rho(\vec{r}))$ is the free-electron exchange potential for the local density $\rho(\vec{r})$. The correlation energy of a uniform electron gas with local density $\rho(\vec{r})$ has been calculated by many authors using different techniques.²²⁻²⁴ The agreement between the most recent results lies within 5–8 mRy in the

metallic density range. Here we use the results of Singwi *et al.*²⁴ fitted to a convenient analytical form²⁵

$$F_{corr}(\rho(\vec{r})) = -A \ln[1 + B\rho^{1/3}(\vec{r})], \quad (7)$$

where $A = 0.0899$ and $B = 33.8518$, in a.u. and similarly

$$\epsilon_c(\rho(\vec{r})) = -C[(1+x^3)\ln(1+1/x) + \frac{1}{2}x - x^2 - \frac{1}{3}], \quad (8)$$

where $\epsilon_c(\rho(\vec{r}))$ is the free-electron correlation potential for local density $\rho(\vec{r})$, with

$$x = r_s/A, \quad \frac{4}{3}\pi r_s^3 = \rho^{-1}(\vec{r}), \quad C = 0.045.$$

The total exchange and correlation energy is given at this level of approximation by

$$E_{xc}(\rho(\vec{r})) \cong \int \rho(\vec{r}) [\epsilon_x(\rho(\vec{r})) + \epsilon_c(\rho(\vec{r}))] d\vec{r}. \quad (9)$$

The LDF formalism has been used in the past with the functionals $F_{ex}(\rho(\vec{r}))$ and $F_{corr}(\rho(\vec{r}))$ to calculate charge densities, total ground-state energies, and ionization potentials for some atoms²⁶ and molecules²⁷ and has yielded reasonably good results. The situation in the area of applying the LDF formalism to realistic solid-state models is rather different. Most of the existing local-exchange one-electron band-structure calculations on solids are based on retaining only the first term in the gradient expansion^{18,19} [namely, the free-electron exchange $\epsilon_x(\rho(\vec{r}))$]. Also, due to additional approximations invoked in order to simplify the solution of the one-particle equation,^{18,20} a meaningful comparison of the predictions of the LDF determined ground-state observables (i.e., total energy, lattice constants, Compton profiles, Fermi-surface data, structure factors, etc.) with

experiment has been hindered. Recent work in the field has demonstrated some dramatic changes in the calculated cohesive energy,¹⁰ Fermi surface,^{28,29} band structure,^{8,11,28} and charge density³⁰ when the simplifying muffin-tin approximation or the lack of self-consistency are relaxed. Of particular interest to us also in the comparison of the predictions of LDF formalism results on some ground-state observables with those obtained by the restricted Hartree-Fock model by Euwema and co-workers.³¹⁻³⁴ In view of this situation, we have undertaken the problem of devising an efficient and reliable method for solving the local-density one-particle equation [Eq. (2)] using the restricted form of the exchange and correlation functional [Eqs. (5)–(8)].

III. BASIC METHODOLOGY

In this section we describe the main features of our method for solving self-consistently the LDF one-particle equation (2) with the functional defined in Eqs. (5)–(9). We will hence discuss the methods used to generate the initial crystal potential, the basis functions, and outline the procedure used to construct the Hamiltonian matrix elements needed to obtain fully self-consistent solutions in Sec. IV.

A. Crystal potential

To construct an initial crystal potential for an iterative SC solution of Eq. (2), one has to guess a charge density $\rho(\vec{r})$. The most convenient choice seems to be the conventional overlapping-atom model in which a superposition density $\rho_{\text{sup}}(\vec{r})$ is constructed from one-center (spherical) charge densities $\rho_\alpha(r, \{f_{nl}, Q^\alpha\})$ in the form

$$\rho^{\text{sup}}(\vec{r}) = \sum_m^N \sum_\alpha^h \rho_\alpha(\vec{r} - \vec{R}_m - \vec{d}_\alpha, \{f_{nl}^\alpha, Q^\alpha\}), \quad (10)$$

where \vec{R}_m and \vec{d}_α denote the position vector of the m th unit cell and α th atomic sublattice site, respectively. N is the number of unit cells and h is the number of atoms in each cell. $\rho_\alpha(\vec{r}, \{f_{nl}^\alpha, Q^\alpha\})$ is the charge density of atom α calculated from some independent theory (Hartree-Fock, LDF formalism, Thomas-Fermi, etc.) assuming the (generally noninteger) atomic occupation numbers f_{nl}^α , for the central field quantum numbers n and l and a possible net ionic charge of Q^α .

Several possibilities exist as to the choice of the one-site charge densities $\rho_\alpha(\vec{r})$ to be used as an initial guess for $\rho^{\text{sup}}(\vec{r})$. Because of the SC requirement, the choice is rather arbitrary and should be made by considering the convergence rate of the SC cycles. We tried a series of procedures for selecting $\rho_\alpha(\vec{r})$ before choosing the one

that seems to work best; we choose $\rho_\alpha(\vec{r})$ as the density obtained from the SC solution of the LDF one-particle equation [Eq. (2)] for an isolated atom:

$$\left(-\frac{1}{2} \nabla^2 - \frac{Z_\alpha}{\vec{r}} + \int \frac{\rho_\alpha(\vec{r}')}{|\vec{r} - \vec{r}'|} d\vec{r}' + F_{\text{ex}}(\rho_\alpha(\vec{r})) + F_{\text{corr}}(\rho_\alpha(\vec{r})) \right) \varphi_{n,l}^\alpha(\vec{r}) = \epsilon_{n,l}^0 \varphi_{n,l}^\alpha(\vec{r}), \quad (11)$$

where $F_{\text{ex}}(\rho_\alpha(\vec{r}))$ and $F_{\text{corr}}(\rho_\alpha(\vec{r}))$ are the exchange and correlation functionals, respectively [Eqs. (6)–(7)], acting on the one-center density $\rho_\alpha(\vec{r})$. Omitting the indices $f_{n,l}^\alpha$ and Q^α from $\rho_\alpha(\vec{r})$, the latter quantity is simply given by

$$\rho_\alpha(\vec{r}) = \sum_{n,l}^{N_{\text{oc}}} f_{n,l}^\alpha |\varphi_{n,l}^\alpha(\vec{r})|^2, \quad (12)$$

where the sum extends to all assumed occupied (core + valence) atomic levels N_{oc} . Equations (11) and (12) are solved self-consistently (using a Herman-Skillman³⁵ type program) for each type of atom appearing in the crystal unit cell assuming a given set of atomic-orbital occupation numbers $f_{n,l}^\alpha$ (generally nonintegers) and ionic charge Q^α . With this choice of $\rho^{\text{sup}}(\vec{r})$, the initial electrostatic potential [second and third terms in Eq. (2)] can be written as a sum of a short-range Coulomb $V_{\text{SRC}}^{\text{sup}}(\vec{r})$ and a long-range Coulomb $V_{\text{LRC}}^{\text{sup}}(\vec{r})$ parts. Because of the linearity of Poisson's equation, the short-range Coulomb crystal potential is expressible as a linear superposition

$$V_{\text{SRC}}^{\text{sup}}(\vec{r}) = \sum_{\vec{R}_m}^{R_{\text{max}}} \sum_{\alpha}^h v_\alpha(\vec{r} - \vec{R}_m - \vec{d}_\alpha), \quad (13a)$$

where the Coulomb potential associated with site α is given by

$$v_\alpha(\vec{r}) = \int \frac{\rho_\alpha(\vec{r}')}{|\vec{r} - \vec{r}'|} d\vec{r}' - \frac{Z_\alpha - Q^\alpha}{\vec{r}}. \quad (13b)$$

Q^α denotes the residual charge that remains unscreened by the electronic one-site charge density $\rho_\alpha(\vec{r})$ when the summation in Eq. (13a) is carried out to a finite range R_{max} ; its magnitude is defined as $\lim_{r \rightarrow R_{\text{max}}} r v_\alpha(r) = Q^\alpha$ as $r \rightarrow R_{\text{max}}$.

In homopolar systems, where the discrete lattice sum in Eq. (13a) is carried out to about 20–25 a.u., Q^α becomes very small (due to the rapid fall-off of the local-density atomic wave functions) and $V_{\text{SRC}}^{\text{sup}}(\vec{r})$ becomes the only significant contribution to the crystal Coulomb potential. When Q^α is larger than some prescribed tolerance ($\sim 10^{-4}e$), the long-range Coulomb potential $V_{\text{LRC}}^{\text{sup}}(\vec{r})$ is calculated using standard Ewald summation techniques.^{36,37} Note that all aspherical contributions originating from the overlapping tails of the one-site potentials $v_\alpha(\vec{r})$, as well as those contributed by the point-ion electrostatic

crystal field $V_{\text{LRC}}^{\text{sup}}(\vec{r})$, are not approximated by their spherically projected part in our initial crystal potential. The superposition exchange and correlation potentials $V_x^{\text{sup}}(\vec{r})$ and $V_{\text{corr}}^{\text{sup}}(\vec{r})$, respectively, are defined by applying the functionals given in Eqs. (6) and (7) to $\rho^{\text{sup}}(\vec{r})$. Owing to the nonlinearity of the local exchange and correlation functional with respect to the individual single-site densities $\rho_\alpha(\vec{r})$, the initial "superposition" potential $V^{\text{sup}}(\vec{r})$ given by

$$V^{\text{sup}}(\vec{r}) = V_{\text{SCR}}^{\text{sup}}(\vec{r}) + V_{\text{LRC}}^{\text{sup}}(\vec{r}) + V_x^{\text{sup}}(\vec{r}) + V_{\text{corr}}^{\text{sup}}(\vec{r}) \quad (14)$$

is not representable as a lattice sum of one-center atomic potentials and hence even at this "zerth iteration" stage, Eq. (2) constitutes a multicenter problem. Many LCAO techniques^{11,13} as well as the multiple-scattering $X\alpha$ (MS $X\alpha$) method³⁸ are possible only if the potential is representable as a sum of single-site terms, in which case either functionals like $F_{\text{ex}}(\rho(\vec{r}))$ are arbitrarily linearized^{3,11} [e.g., $V_x(\vec{r})$ is set to $\sum_m \sum_\alpha F_{\text{ex}} \times (\rho_\alpha(\vec{r} - \vec{R}_m - \vec{d}_\alpha))$] or the superposition potential is spherically averaged around each atomic site.^{6,7} The consequences of these rather drastic approximations on some calculated observables have been discussed previously.^{8,10,29,30} As an alternative to these approximations, one might project numerically each of the term in V^{sup} and $\rho^{\text{sup}}(\vec{r})$ onto an analytic single-site basis^{14,15} using least-squares techniques. Although possible, such an approach requires a separate auxiliary basis set to be devised for fitting each of the terms in V^{sup} , and this becomes almost intractable when the function to be fitted contains high central-field l components. In previous attempts,¹⁵ it was also demonstrated that when complicated quantities like the total energy are to be calculated, small fitting errors [mainly in the steep part of $V_x^{\text{sup}}(\vec{r})$] produce large numerical instabilities in the calculated observables. Since no use is made in this work of a potential function that is linear in the one-site contributions, none of these approximations is necessary. In particular, the potential is allowed to have the full site symmetry required by the crystal structure in question [i.e., in the language of perturbative corrections to muffin-tin method,³⁹ $V^{\text{sup}}(\vec{r})$ includes both "exact" warping and allows for nonspherical components inside "atomic spheres"]. After the convergence of the direct lattice sums [Eqs. (10) and (13a)] is maintained (to a tolerance of 10^{-8} a.u. in the potential), our initial $V^{\text{sup}}(\vec{r})$ is fully defined by specifying Z_α , the postulated crystal structure, and the assumed $\{f_{n,l}^\alpha\}$ and charges $\{Q^\alpha\}$ used to construct $\rho_\alpha(\vec{r})$. The latter two will be treated as essentially free

parameters in the SC procedure to produce the "best" superposition potential.

Figure 1 displays three-dimensional plots of the superposition Coulomb, exchange, and correlation potentials for diamond in the $(1\bar{1}0)$ plane⁴⁰; they all follow the essential pattern of the input charge density. Nonconstant regions in the "intersphere" Coulomb, exchange and correlation parts are easily visible (especially in the exchange and correlation parts). A lattice constant of 6.742 a.u. was used and an input $1s^2 2s^2 2p^2$ electronic configuration is assumed. The exchange potential constitutes some 55% of the Coulomb potential in the interstitial region while the correlation potential has smaller values (5%) in that region.

B. Basis functions

As is usual in Roothaan-type variational treatments, the crystal eigenfunction $\psi_j(\vec{k}, \vec{r})$ (band index j and translational representation \vec{k}) is expanded in terms of $h\eta$ Bloch functions, $\Phi_{\mu\alpha}(\vec{k}, \vec{r})$, in a standard fashion:

$$\psi_j(\vec{k}, \vec{r}) = \sum_{\alpha=1}^h \sum_{\mu=1}^{\eta} C_{\mu\alpha j}(\vec{k}) \Phi_{\mu\alpha}(\vec{k}, \vec{r}). \quad (15)$$

Here $\Phi_{\mu\alpha}(\vec{k}, \vec{r})$, defined in terms of the μ th basis function on the α th sublattice, $\chi_\mu^\alpha(\vec{r})$ is given by

$$\Phi_{\mu\alpha}(\vec{k}, \vec{r}) = N^{-1/2} \sum_{m=1}^N e^{i\vec{k}\cdot\vec{R}_m} \chi_\mu^\alpha(\vec{r} - \vec{R}_m - \vec{d}_\alpha), \quad (16)$$

and $\{\chi_\mu^\alpha(\vec{r}), \mu = 1, \dots, \eta; \alpha = 1, \dots, h\}$ constitutes the elementary basis set. A central problem is the choice of an optimum basis. One desires a large linearly independent basis set so as to main-

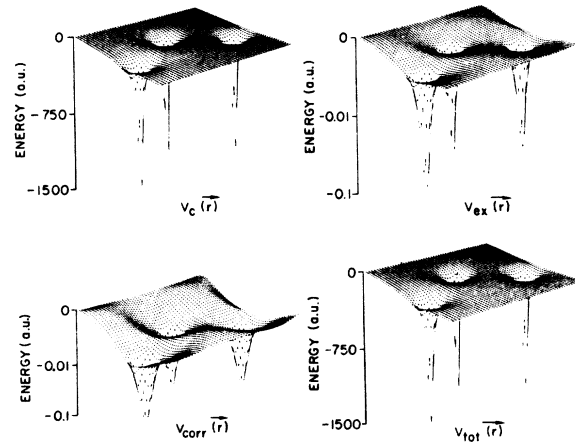


FIG. 1. Three-dimensional plots of the various components of the superposition potential in the $(1\bar{1}0)$ plane. Singular potentials are denoted by vertical dashed lines at the atomic site.

tain sufficient variational freedom throughout the Brillouin zone (BZ). A minimal basis set could lead to the expansion coefficients $C_{\mu\alpha j}(\mathbf{k})$ being completely determined by symmetry for some high-symmetry states in the BZ. However, since the number of Hamiltonian matrix elements increases rapidly with the size of the basis set, an unduly large set is to be avoided. Obviously, the basis set convergence rate of calculated observables can be made to be rapid when the basis functions are carefully chosen to be compatible with the type of Hamiltonian to be solved. One would require that the basis set be flexible enough to adequately describe the various regions in the real space unit cell (oscillatory nodal behavior near the atomic sites with the appropriate Coulomb cusps at the position of the nuclei and spatially smooth in the bonding interatomic region) and various energy eigenvalue ranges (deep core states, valence, and excited states). [Note that while in nonperiodic polyatomic systems one may need both short- and long-range basis functions to describe the various regions in the molecule, in periodic systems the latter are both numerically inconvenient (due to the need to perform long-range lattice sums), and, in many cases, variationally unimportant (since Bloch functions formed from short- or medium-range basis functions already span an arbitrarily long range).]

While band structure methods (e.g., "conventional" APW, Korringa-Kohn-Rostoker and cellular schemes) that rely heavily on approximating the multicenter crystal potential with its aspherical site symmetry by sums of one-center terms having a one-dimensional radial site symmetry can utilize a conveniently convergent representation for the eigenfunctions (one-site partial waves, plane waves, etc.), band methods that do not restrict the form of the crystal Hamiltonian are usually forced to resort to somewhat artificial analytic functions to ease the difficulty of computing multicenter integrals. Past experience with these basis functions (Slater orbitals, Gaussians, etc.) in quantum chemical molecular computations⁴¹ has frequently revealed, along with a reasonable convergence of one-electron eigenvalues with respect to basis set size, a rather slow convergence of calculated many-electron observables like the total energy. Since no use is made in the method described in this paper of any analytical or semianalytical algorithm for calculating the Hamiltonian matrix elements, we are free to choose a general basis set with which to meet the considerations for an optimum set discussed above. The criteria used for selecting a given expansion set were its compactness and variational efficiency in lowering the ground-state

total energy.⁴² Our basis set contains functions that are conveniently classified into three types: (a) "Exact" self-consistent LDF numerical orbitals for the occupied and lowest virtual levels of the atoms appearing in the crystal unit cell. (b) Additional "free" uncontracted Slater-type orbitals spanning the virtual space. (c) "Ion-pair" charge transfer functions, e.g., numerical atomic orbitals associated with a negatively and with a positively charged atom.

The "exact" self-consistent (LDF) numerical orbitals are directly calculated by numerical integration of the central-field atomic one-particle equation in the LDF formalism:

$$\left[-\frac{1}{2}\nabla^2 + g_\alpha(r)\right]\chi_{n,l}^\alpha(r; \{f_{n',l'}, Q^\alpha\}) = \epsilon_{n,l}^\alpha \chi_{n,l}^\alpha(r; \{f_{n',l'}, Q^\alpha\}). \quad (17)$$

In this equation, $\epsilon_{n,l}^\alpha$ are the atomiclike eigenvalues and $\chi_{n,l}^\alpha(r; \{f_{n',l'}, Q^\alpha\})$ denote the atomiclike radial orbitals for level n, l (for atom of type α) that depend parametrically on the prescribed population numbers $f_{n',l'}$, of all N_{oc} occupied levels in the atom (the m degeneracy in central fields being averaged) and on the net atomic charge Q^α . The net atomic charge is simply related to the nuclear charge Z_α and the electronic populations $f_{n,l}$ by

$$Q^\alpha = Z_\alpha - \sum_{n,l}^{N_{oc}} f_{n,l}. \quad (18)$$

The one-site potential $g_\alpha(r)$ can be any generalized atomiclike potential, as long as it generates via Eq. (17) eigenfunctions that form a convenient and rapidly convergent basis set for expanding the crystal orbitals. We would like them to be atomiclike near the atomic site, so as to be compatible with the crystal potential in these regions; however, the long-range nature of the free-atom eigenfunctions should be controlled in order to avoid linear dependence between the Bloch functions generated from them. The oscillations generated by the nodal character of the full (core + valence) atomic functions as well as the characteristic cusp of an exact atomic solution at the nucleus are desirable in order to partially cancel the Coulomb singularity in the crystal potential by the appropriate repulsive kinetic-energy terms. The one-site potential $g_\alpha(r)$ is accordingly chosen as a slightly modified atomic local-density potential:

$$g_\alpha(r) = V_{\text{Coul}}^\alpha(r) + V_{\text{ex}}^\alpha(r) + V_{\text{corr}}^\alpha(r) + A(r), \quad (19)$$

where $V_{\text{Coul}}^\alpha(r)$, $V_{\text{ex}}^\alpha(r)$, and $V_{\text{corr}}^\alpha(r)$ are derived from the total single-site ground-state charge density

$$\eta_\alpha(r) = \sum_{n,l}^{N_{oc}} f_{n,l}^\alpha [\chi_{n,l}^\alpha(r; \{f_{n',l'}, Q^\alpha\})]^2 \quad (20)$$

through the usual α th-site Poisson equation and the local density exchange and correlation functionals [Eqs. (6) and (7)].

The additional term $A(r)$ is a prescribed external potential chosen to tailor the $\chi_{n,i}^\alpha$ for their use as basis functions in the crystalline variational calculation. Again, several choices are reasonable: in order to obtain basis functions that are less diffuse than are "free" atomic orbitals, one might choose for $A(r)$ a Latter tail correction⁴⁴ with a suitable coefficient that has the effect of compressing the long-range orbitals tails, an external potential well^{45,46} or to adopt the Adams-Gilbert term,⁴⁷ modified for local potentials, to generate more localized (and self-consistent) central-field single-site orbitals. Note that we attach no physical meaning to the $\epsilon_{n,i}^0$, and that Eq. (17), which is used only to generate basis functions, is solved numerically in a SC manner after prescribing a fixed set of (noninteger) $f_{n,i}^\alpha$ and Q^α . Thus, the single-site potential $g_\alpha(\vec{r})$ used to generate the numerical basis orbitals is not restricted to be equal to the potential used to generate the model superposition density [Eqs. (11) and (12)]. No attempt is made to fit the resulting orbitals to any analytical form (e.g., Slater or Gaussian orbitals); instead, they are used directly in tabular form in the crystalline variational calculation. Such fittings (of double-zeta quality, or so) frequently fail to accurately reproduce the cusps of the exact wave functions and result in considerable errors in the calculation of the large kinetic-energy terms near the nuclei.

It is perhaps worth noting that the initial superposition potential employed in our scheme is already approximately self-consistent with respect to the variational numerical basis set used in the crystal calculation, since the latter solves the one-site eigenvalue equation. In other LCAO-type calculations^{8,9,11-13} the superposition potential is generally unrelated to the basis set, but rather to an independent atomic model (e.g., Hartree-Fock model for the basis functions and a local-density potential).

The numerical basis set is subsequently optimized nonlinearly in the variational calculation in the solid, by recomputing these orbitals from Eq. (17) on the basis of a different $\{f_{n,i}^\alpha, Q^\alpha\}$ set chosen from a charge analysis of the *crystalline* wave functions throughout the BZ. The basis functions are thus allowed to relax *nonlinearly* (and iteratively) to the crystal potential, thereby increasing their variational flexibility. Formerly virtual atomic states are thus allowed to become fractionally populated according to their variational participation in the ground-state crystal eigenfunctions and subsequently become much more localized.

The *minimal* numerical atomiclike basis set forms a very compact and flexible basis, whose quality, as estimated from previous molecular calculations⁴⁶ and from our own experience,³⁰ is comparable at least to that of a double-zeta Slater set. In this paper, we use both a minimal (1s, 2s, 2p numerical orbital for second-row atoms) and an extended numerical set (with the addition of 3s, 3p, and 3d numerical orbitals). In each case, the Bloch functions formed from the basis functions are Löwdin orthogonalized⁴⁸; linearly dependent functions that result in eigenvalues of the overlap matrix (in the Bloch representation) which are smaller than a prescribed tolerance of 10^{-2} , are automatically discarded (i.e., a canonically orthogonalized set⁴⁸ is used). Whenever inclusion of higher virtual states seems desirable, but becomes impossible due to linear dependence, the numerical set is augmented by type-(b) basis functions whose exponents are adjusted so that the maximum of each orbital falls within the Wigner-Seitz cell. These orbitals are then treated in an identical manner as the numerical orbitals except for the analytic evaluation of the kinetic-energy matrix elements.

The combination of basis functions of type (a) and (b) seems to constitute an excellent set as far as one-electron eigenvalues are concerned. Essentially no further changes are observed in the valence and low-lying conduction-state eigenvalues (only states below $E_F + 15$ eV are examined) in the materials studied so far (diamond, BN, LiF, Ne, TiS₂) after a minimal numeric set is augmented by the first two or three virtual states. The situation is, however, different when the total energy is considered where, e.g., for diamond, a major improvement is obtained by adding an ion-pair basis set [type (c)] to the usual numerical set. In this case we solve the atomiclike one-site equation [Eq. (17)] not only for neutral carbon ($Q^\alpha = 0$) but also for the ionic configurations $1s^2 2s^1 2p^{3+Q}$ having a net charge of Q and $-Q$, and use this triple-size set to construct our Bloch functions. Experimentation with this type of set revealed that the results are not too sensitive to the value of $|Q|$ around 0.8–1.0 and that the best total energy seems to occur for $Q = \pm 0.85$.

Figure 2 displays three-dimensional plots of the optimized numeric Bloch functions in the (110) plane in diamond [converged to within one part in 10^4 with respect to the lattice sums and the accuracy in the solution of Eq. (17) is 1 part in 10^6]. These are obtained by generating the numerical one-site functions from a self-consistent solution of Eq. (17) with a Latter tail taken as $A(r)$ and using an electronic configuration of $1s^2 2s^2 2p^2 3s^0 3p^0 3d^0$ and superposing the contri-

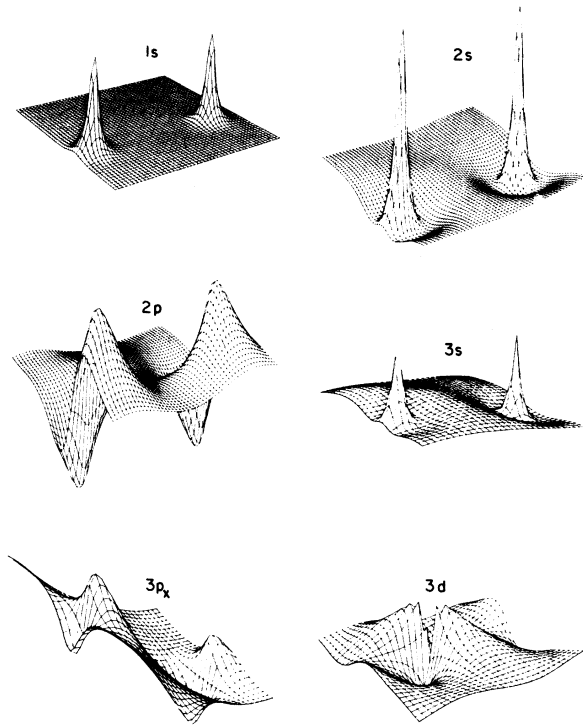


FIG. 2. Three-dimensional plots of the numerical Bloch functions at the Γ point in the BZ ($1\bar{1}0$).

butions from various unit cells to yield $\Phi_{\mu\alpha}(\vec{k}, \vec{r})$ as indicated in Eq. (16).

C. Matrix elements

Once the model initial potential $V^{\text{sup}}(\vec{r})$ and the expansion basis set are defined, the usual linear-variation secular matrix

$$\sum_{\alpha=1}^h \sum_{\mu=1}^n [H_{\mu\alpha, \nu\beta}(\vec{k}) - S_{\mu\alpha, \nu\beta}(\vec{k}) \epsilon_j(\vec{k})] C_{\mu\alpha j}(\vec{k}) = 0 \quad (21)$$

is solved, where the Hamiltonian matrix elements are

$$H_{\mu\alpha, \nu\beta}(\vec{k}) = \langle \Phi_{\mu\alpha}(\vec{k}, \vec{r}) | -\frac{1}{2}\nabla^2 + V(\vec{r}) | \Phi_{\nu\beta}(\vec{k}, \vec{r}) \rangle, \quad (22)$$

and the overlap matrix elements

$$S_{\mu\alpha, \nu\beta}(\vec{k}) = \langle \Phi_{\mu\alpha}(\vec{k}, \vec{r}) | \Phi_{\nu\beta}(\vec{k}, \vec{r}) \rangle. \quad (23)$$

The eigenvalue spectrum $\epsilon_j(\vec{k})$ yields the band structure defined throughout the BZ; however, since they are found strictly from ground-state local-density operators defining $V(\vec{r})$, they bear no rigorous relation to elementary excitations in the system.

In order to achieve maximum flexibility in the construction of $V(\vec{r})$ [e.g., by including arbitrary

forms for the correlation part and avoiding linearization of $F_{\text{ex}}(\rho^{\text{sup}}(\vec{r}))$ and $F_{\text{corr}}(\rho^{\text{sup}}(\vec{r}))$, etc.] and the $\Phi_{\mu\alpha}(\vec{k}, \vec{r})$ (e.g., by allowing for nonanalytic and possible off-center basis functions) one has to have a general form-independent algorithm for calculating the three-dimensional multicenter integrals appearing in Eqs. (22) and (23).

Figures (1) and (2), showing the shapes of $V(\vec{r})$ and $\Phi_{\mu\alpha}(\vec{k}, \vec{r})$, reveal the fact that any integration scheme with this type of integrands must be able to cope with the Coulomb singularities in $V(\vec{r})$ the nodal character of $\Phi_{\mu\alpha}(\vec{k}, \vec{r})$ near the nuclei and their diffuse shape in the interstitial region. Contrary to the situation met in problems of integrating the three-dimensional corrections to the muffin-tin charge density,¹⁰ the integrands encountered in our problem are continuous throughout the integration space. Also, unlike the situation occurring in *molecular* three-dimensional integrations,^{14,15} we do not have to treat both the interatomic and the "outer-molecular" tails of the integrands, since our integration is confined to a single unit cell and the integrands do not fall off to very small numerical values. Guided by these considerations we have adopted the three-dimensional Diophantine numerical integration scheme, developed by Haselgrove¹⁶ and Conroy⁴⁹ and adapted to molecular¹⁴ and solid state^{8,9} problems by Ellis and co-workers. The method defines a set of pseudorandom integration sampling points $\{\vec{r}_i\}$ inside a unit cell and an associated set of weight function $\{w(\vec{r}_i)\}$ together with a tabular form of the integrand, to yield

$$\int d\vec{r} \Phi_{\mu\alpha}(\vec{k}, \vec{r}) V(\vec{r}) \Phi_{\nu\beta}(\vec{k}, \vec{r}) \cong \sum_{i=1}^M w_i(\vec{r}_i) \Phi_{\mu\alpha}(\vec{k}, \vec{r}_i) V(\vec{r}_i) \Phi_{\nu\beta}(\vec{k}, \vec{r}_i). \quad (24)$$

The convergence properties of this scheme has been subject to numerous discussions in the literature^{8,9} and will not be repeated here. With numerical Bloch functions and a multicenter crystal potential, the sampling that seems to work best is based on a linear superposition of functions of the form

$$w(\vec{r}_i) \sim \sum_{\alpha} |\vec{r}_i - \vec{d}_{\alpha}|^2 \quad (25)$$

centered on each atomic site α , a Gaussian distribution of sampling points centered at the middle of each bond, and a constant density of points everywhere else. This importance sampling treats the Coulomb singularities efficiently by making the function $w(\vec{r}_i)H(\vec{r}_i)$ relatively smooth even at the position of the nuclei and takes care

of the buildup of charge in the bond region. The method is very simple and straightforward to use and provides a typical convergence, using 2000 sampling points, of 1 mRy or less for the valence-band structure in diamond and 2 mRy for the first four conduction bands. (Similar convergence rates have been obtained for Li, cubic boron nitride, LiF, and Ne.) For a typical transition-metal compound like TiS₂, around 5000 integration points were required to achieve an over-all 1–3-mRy convergence in the region below $\epsilon_F + 15$ eV. The convergence of the total energy and the Compton profile is somewhat slower, and will be discussed later.

The direct integration of Eqs. (22) and (23) avoids the difficult multicenter integrals appearing in Roothaan-type LCAO expansions.^{11–13} By using a carefully chosen $\omega_i(\vec{r}_i)$ in Eq. (24) to smooth out the Coulomb singularities, all energy integrals are treated accurately in a real-space representation and the usual difficulties in treating the slowly convergent Fourier expansion of such potentials in reciprocal-space techniques^{50–52} (where some 20 000 reciprocal-lattice vectors were typically needed to obtain reasonable convergence⁵⁰)

are avoided. We note that the method is capable of treating general terms in $V(\vec{r})$ (i.e., various functional forms of local exchange and correlation) without having to introduce additional fit functions (such as are used in Gaussian-transform techniques^{11, 15, 52} to project the multicenter potential into a form that is linear in the contributions originating from each center)—procedures which not only require a different projection set for each density functional appearing in the Hamiltonian, but also tend to require a large auxiliary fitting basis set when the ground-state density includes large l components.

The calculation of both the Hamiltonian matrix elements and the total crystal energy in models that consider the full (core + valence) electron contribution to the Hamiltonian is fraught with the well-known difficulty of having to deal with small differences between the large repulsive kinetic-energy terms and attractive potential terms in the neighborhood of the atomic cores. The use of exact numerical atomic orbitals provides a straightforward simplification of that problem.

The (initial) crystal Hamiltonian operating on $\Phi_{\mu, \alpha}(\vec{k}, \vec{r})$ yields [using Eqs. (16) and (17)]

$$H\Phi_{\mu, \alpha}(\vec{k}, \vec{r}) = V(\vec{r})\Phi_{\mu, \alpha}(\vec{k}, \vec{r}) + T\Phi_{\mu, \alpha}(\vec{k}, \vec{r}) = [V_{\text{SRC}}^{\text{sup}}(\vec{r}) + V_x^{\text{sup}}(\vec{r}) + V_{\text{LRC}}^{\text{sup}}(\vec{r}) + V_{\text{corr}}^{\text{sup}}(\vec{r})]\Phi_{\mu, \alpha}(\vec{k}, \vec{r}) + \sum_m e^{i\vec{k}\cdot\vec{R}_m} \chi_{\mu}^{\alpha}(\vec{r} - \vec{R}_m - \vec{d}_{\alpha}) [\epsilon_{\mu}^{\circ} - g_{\alpha}(\vec{r} - \vec{R}_m - \vec{d}_{\alpha})]. \quad (26)$$

If $T\Phi_{\mu, \alpha}(\vec{k}, \vec{r})$ is combined numerically with $\frac{1}{2}V(\vec{r})\Phi_{\mu, \alpha}(\vec{k}, \vec{r})$ (the factor of $\frac{1}{2}$ originates from the detailed consideration of the real and imaginary parts of the appropriate functions) *before* integration of $\Phi_{\nu, \beta}(\vec{k}, \vec{r})[H\Phi_{\mu, \alpha}(\vec{k}, \vec{r})]$ is attempted, the attractive Coulomb singularity in $V_{\text{SRC}}^{\text{sup}}(\vec{r})$ near the α th core is effectively cancelled by the kinetic-energy term having a repulsive $-g_{\alpha}(\vec{r} - \vec{R}_m - \vec{d}_{\alpha})$ dependence. Thus, to the extent that the charge density arising from orbital χ_{μ}^{α} contributes to the ground-state Coulomb potential in $V^{\text{sup}}(\vec{r})$ [Eqs. (12) and (13)], it would act to cancel the positive kinetic energy arising from the same center. This cancellation is expected to be effective only if the $\Phi_{\mu, \alpha}(\vec{k}, \vec{r})$ are formed from exact eigenvectors of the operator $[g_{\alpha}(\vec{r}) - \frac{1}{2}\nabla^2]$ and if the Coulomb singularities in $V^{\text{sup}}(\vec{r})$ are formed from the superimposed Coulomb parts in $g_{\alpha}(\vec{r})$.^{53, 54} This is so both at the initial step in our SC cycle, where $V^{\text{sup}}(\vec{r})$ contains a superposition of the Coulomb part of $g_{\alpha}(\vec{r})$, and at an arbitrary SC iteration where the basis orbitals $\chi_{\mu}^{\alpha}(\vec{r})$ are nonlinearly optimized along with identical changes being carried for $g_{\alpha}(\vec{r})$ and $V_{\text{SRC}}(\vec{r})$. Obviously,

orbitals which are used to construct Bloch states that are not related to the one-site potential $g_{\alpha}(\vec{r})$ (e.g., Slater orbitals, virtual states of $g_{\alpha}(\vec{r})$, etc.) do not contribute to the cancellation between $V(\vec{r})\Phi_{\mu, \alpha}(\vec{k}, \vec{r})$ and $T\Phi_{\mu, \alpha}(\vec{k}, \vec{r})$. It is usually sufficient, however, to have the low-lying core states (1s, 2s) participate in $g_{\alpha}(\vec{r})$ and $V(\vec{r})$ and to use the appropriate exact orbitals in the Bloch basis to obtain a satisfactory cancellation in the integrands. The numerical Diophantine integration is then applied to integrate $\Phi_{\mu, \alpha}(\vec{k}, \vec{r})[H\Phi_{\nu, \beta}(\vec{k}, \vec{r})]$ *after* the cancellation in the integrand was allowed to occur algebraically.

Figure 3 shows three-dimensional plots of the functions $T\Phi_{\mu, \alpha}(\vec{k}, \vec{r})$, and $V^{\text{sup}}(\vec{r})\Phi_{\mu, \alpha}(\vec{k}, \vec{r})$ in the (110) plane of diamond at the Γ point ($\vec{k}=0$) for some representative Bloch functions. The large cancellation between the kinetic and potential terms near the cores (note the different scales), especially for the 1s Bloch state, is apparent. Note that a similar, but usually arbitrary, cancellation in the basis of the pseudopotential method and is the cause of its success.

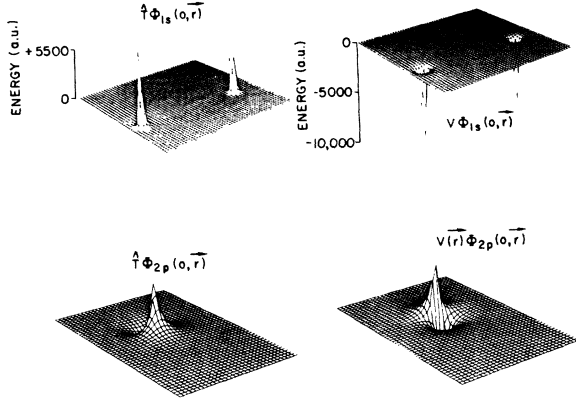


FIG. 3. Three-dimensional plots of $\hat{T}\Phi_{\mu}(0, \vec{r})$ and $V^{\text{sup}}(\vec{r})\Phi_{\mu}(0, \vec{r})$ for the Bloch states $1s$ and $2p$, in the $(1\bar{1}0)$ plane. Singular functions are denoted by the vertical dashed lines at the atomic site.

IV. SELF-CONSISTENCY

A. General considerations

The solution of the LDF problem for an assumed model $\rho^{\text{sup}}(\vec{r})$ [Eq. (10)] provides us with $\psi_j(\vec{k}, \vec{r})$ that define the crystal density $\rho_{\text{cry}}(\vec{r})$ as

$$\rho_{\text{cry}}(\vec{r}) = N \frac{\Omega}{(2\pi)^3} \sum_{j=1}^{\sigma_{\text{oc}}} \int_{\text{OBZ}} [n_j(\vec{k}) \psi_j^*(\vec{k}, \vec{r}) \psi_j(\vec{k}, \vec{r})] d\vec{k}, \quad (27)$$

when the sum extends over all σ_{oc} bands spanning the occupied volume of the Brillouin zone (OBZ) and Ω denotes the unit-cell volume. The occupation numbers $n_j(\vec{k})$ are chosen according to the Fermi statistics (for states lying on the Fermi surface, a fractional population is possible). The integration in Eq. (27) is performed by choosing a discrete number of points in \vec{k} space and an associated set of weight functions $\omega_j(\vec{k})$ chosen according to the nearest volume algorithm. We have used 4, 6, and 19 points in the $\frac{1}{48}$ irreducible section of the BZ (or 14, 32, and 256 in the full zone, respectively) and have examined the convergence of some of the calculated observables with respect to the number of sampling points. The results presented in Sec. VB indicate the contrary to objections raised^{50, 55} previously, the dispersion of the bracket terms in Eq. (27) is usually small enough for good results to be obtained even with the six nearest-volume points. Hence, we use

$$\rho_{\text{cry}}(\vec{r}) \cong N \frac{\Omega}{(2\pi)^3} \sum_{\vec{k}_{\alpha}} \sum_{j=1}^{\sigma_{\text{oc}}} \omega_j(\vec{k}_{\alpha}) n_j \times (\vec{k}_{\alpha}) \psi_j^*(\vec{k}_{\alpha}, \vec{r}) \psi_j(\vec{k}_{\alpha}, \vec{r}), \quad (28)$$

where $\omega_j(\vec{k}_{\alpha})$ are weights that become j indepen-

dent in systems having no Fermi surface and are chosen according to the Chadi and Cohen⁵⁶ algorithm as generalized by Monkhorst and Pack.⁵⁷ In this way $\rho_{\text{cry}}(\vec{r})$ is calculated in tabular form for 2000–3000 points in the unit cell.

Since Eq. (2) yields variational solutions only if the eigenvectors ψ_j are consistent with the charge density determining the value of the functional in this equation, one has obviously to perform a SC calculation in order to obtain meaningful results. Since the term “self-consistency” has been used rather loosely in some previous band-structure calculations (in that severe restrictions were imposed on the SC path) we discuss various possible degrees of SC along with our particular method for obtaining “full” SC. We will thereby distinguish between charge and configuration self-consistency (CCSC is stage 1 in SC) and full self-consistency (FSC is stage 2 in SC).

The major difficulty in obtaining FSC with $\rho_{\text{cry}}(\vec{r})$ given in Eq. (28) is related to the problem of having to obtain the Coulomb part of the potential by solving the Poisson equation and to generate the refined exchange and correlation potentials for the next iteration. While the model density $\rho^{\text{sup}}(\vec{r})$ is expressed as a lattice sum of one-center contributions for which the associated Coulomb potential is readily found, the output crystal density $\rho_{\text{cry}}(\vec{r})$ is a multicenter function which is not expressible in terms of one-center atomic densities located on atomic sites.

In what follows, we define CCSC as a consistent relation between $V_{\text{cry}}(\vec{r})$ and $\rho_{\text{cry}}(\vec{r})$ in which we limit the crystal density to *sums of one-center terms located on existing atomic sites*. In this approach

$$\rho_{\text{cry}}(\vec{r}) \cong \rho_0(\vec{r}) = \sum_{m=1}^N \sum_{\alpha=1}^h \sum_i a_i \rho_i(\vec{r} - \vec{R}_m - \vec{d}_{\alpha}) \quad (29)$$

at each iteration step where a_i and ρ_i denote the expansion coefficients and the fitting functions, respectively. It is to be understood that depending on the degree of approximation involved in simulating $\rho_{\text{cry}}(\vec{r})$ by $\rho_0(\vec{r})$, there will always exist a residual density

$$\Delta\rho(\vec{r}) \equiv \rho_{\text{cry}}(\vec{r}) - \rho_0(\vec{r}) \quad (30)$$

that is not amenable to fitting by single-site basis functions located on atomic sites. Although the form of Eq. (29) makes the problem of calculating the refined crystal potential rather trivial [e.g., when the Poisson equation associated with the individual $\rho_i(\vec{r})$ is solvable analytically of semi-analytically], a SC cycle based on the restriction Eq. (29) may lead in the general case to conver-

gence to an arbitrary limit, depending on the approximations inherent in Eq. (29).

Since a direct real-space point-by-point numerical integration of the multicenter three-dimensional Poisson equation related to $\rho_{\text{cry}}(\vec{r})$ is too laborious to be of practical use, various methods have been devised to circumvent this problem. These are broadly divided into LCAO techniques treating the potential in a reciprocal space⁵⁰⁻⁵² or in a real-space representation.^{14, 15, 58-60} The real-space techniques are usually based on various model assumption for $\rho_0(\vec{r})$ in Eq. (29) [and analogous expressions for $\rho_0^{1/3}(r)$]. Thus, in the multiple-scattering $X\alpha$ (MS $X\alpha$) method⁵⁸ (and associated Korringa-Kohn-Rostoker techniques) one projects $\rho_{\text{cry}}(\vec{r})$ onto a nonoverlapping muffin-tin single-site spherical basis. Although the nonspherical components can be later restored to different degrees of accuracy by using various warping techniques,⁶¹ perturbative multipole expansion corrections,^{29, 62} point-ion corrections⁶³ or by applying a direct perturbation in terms of the non-muffin-tin charge,^{10, 28} these procedures tend to become intractable, especially when iterated towards SC. Various choices of single-site (overlapping) $\rho_i(\vec{r})$ functions have been made in LCAO- $X\alpha$ types of calculations, e.g., contracted Gaussians,¹⁵ single Slater orbitals,¹⁴ angular-dependent functions of the form $C_{lm}(r)Y_{lm}(\theta, \Phi)$,⁵² regular power series in r ,⁶⁴ etc. In the molecular discrete variational method of Ellis *et al.*⁵⁹ and in various forms of the iterative-extended Hückel method⁶⁰ the a_i 's are chosen as Mulliken gross populations,⁶⁵ or Löwdin charges,⁶⁶ and the $\rho_i(\vec{r})$ are simply the atomic densities. Since in all these methods $\Delta\rho(\vec{r})$ is neglected and the convergence to SC is judged by an *internal* criterion within the specific superposition model (e.g., convergence of the Mulliken charges between iterations) it seems difficult to estimate the true degree of SC in these methods.

In the reciprocal space representations,⁵⁰⁻⁵² one expands $\rho_{\text{cry}}(\vec{r})$ in a Fourier series and obtains the Coulomb potential in real space as a sum of reciprocal-lattice vectors (RLV) of the plane-wave modulated Fourier components of $\rho_{\text{cry}}(\vec{r})$. Thus, the difficulties of solving the Poisson equation in a real-space representation are replaced by the problems of having (a) to Fourier transform $\rho_{\text{cry}}(\vec{r})$ [and similarly $\rho_0^{1/3}(\vec{r})$], and (b) to converge the reciprocal-lattice sum on $\rho_{\text{cry}}(\vec{r})$. In the first task, one is again faced with the difficulty of having to perform integrations on the three-dimensional multicenter function $\rho_{\text{cry}}(\vec{r})$ and is resolved either by resorting to a one-center superposition model for^{12b, 52} $\rho_{\text{cry}}(\vec{r})$ or by restricting the basis functions to Gaussians^{50, 51} [in which case the three-

center integrals associated with the Fourier transform of $\rho_{\text{cry}}(\vec{r})$ are computed semianalytically]. In the latter case, the iterated *exchange* potential is either expanded in a (highly truncated) geometrical series,⁵⁰ or the lattice sum of one-site densities $\rho_0(\vec{r})$ is spherically averaged over the unit cell to reduce the Fourier transform of $\rho_0^{1/3}(\vec{r})$ to a one-dimensional integral.^{51b} The validity of these approximations is difficult to assess, especially in systems such as covalently bonded solids which maintain a considerable charge buildup in the interatomic region. All the methods that use reciprocal-space techniques to calculate the iterated crystal potential and incorporate directly both the core and the valence electron contributions on the same footing⁵⁰⁻⁵² face the common difficulty (b) of having to treat a slowly convergent Fourier sum. Owing to the Coulomb singularities in the potential and the sharp features of the core charge density, the convergence of such sums is known to be extremely poor and, unless special procedures are used to accelerate the convergence,⁶⁷ some 10 000–30 000 RLV have been required for reasonable convergence.⁵⁰

In view of these considerations, it seems reasonable to construct a SC scheme in which the advantages offered by a real-space superposition approach (in avoiding the slowly convergent Fourier sums and facilitating the solution of the Poisson equation for the crystal density) are coupled with the efficiency in which three-dimensional multicenter contributions to the potential (that are not expressible within the superposition model) are treated by reciprocal space techniques.

B. Charge and configuration self-consistency

Since there exist an unlimited number of ways of partitioning $\rho_{\text{cry}}(\vec{r})$ into lattice sums of single-site terms [the goal of CCSC being to minimize $\Delta\rho(\vec{r})$ over space], the relevant criteria for choosing a particular partitioning set are efficient in representing $\rho_{\text{cry}}(\vec{r})$, a possible physical significance of the projection set and the degree to which the particular choice facilitates the following stage of "full" SC. Our choice of the partitioning scheme is the superposition model in which the projection set is simply the one-site population-dependent charge densities

$$\rho_0(\vec{r}) = \sum_{m=1}^N \sum_{\alpha=1}^h \sum_{n,l} f_{n,l} [\chi_{n,l}^{\alpha}(\vec{r} - \vec{R}_m - \vec{d}_{\alpha}, \{f_{n',l'}, Q^{\alpha}\})]^2. \quad (31)$$

We thus vary iteratively the "population numbers" $f_{n,l}^{\alpha}$ to minimize, in the least-squares sense, the deviation

$$\sigma^2 = \frac{1}{\Omega} \int \Delta\rho(\vec{r})^2 d\vec{r}. \quad (32)$$

Using this choice, we retain the “self-consistent” relation between the crystal potential and the numerical basis set; this not only facilitates the desired algebraic cancellation between the large kinetic- and potential-energy terms discussed above but also avoids the use of an extra auxiliary fitting-set.^{14,15,52} This choice also provides a natural way to introduce nonlinear variational flexibility into the basis set, by recomputing the one-site orbitals [Eq. (17)] $\chi_{n,i}^\alpha(\vec{r}; \{f_{n,i}^\alpha, Q^\alpha\})$ on the basis of the refined populations and atomic charges $\{f_{n,i}^\alpha, Q^\alpha\}$, thereby allowing them to relax to the current form of the iterated potential. We thus vary nonlinearly the numerical Bloch set on the basis of the populations determined by the requirement of maximum similarity between $\rho_0(\vec{r})$ and $\rho_{\text{cry}}(\vec{r})$. As it turned out, a nonlinear variation of the basis set proved to be necessary only when substantial fractional electronic populations were promoted into previously unpopulated (virtual) orbitals. Under these circumstances, recalculation of the atomic SC orbitals yielded much more contracted orbitals for the formerly virtual states thus rendering them useful in the crystalline variational calculation. By contrast, ordinary atomic virtual orbitals are discarded from the basis set when linear-dependence problems caused by their diffuse nature become severe. Since such charge promotions do not occur in every iteration, it is necessary to regenerate an optimized numerical set only after several iterations. Thus, this scheme also provides us with the possibility of choosing among all atomic superposition models and exact numerical basis functions, the “best” set (in the least-squares sense) for a given crystal, to be used as a reasonable “guess” in future non-self-consistent calculations.

In a typical CCSC iteration, we compute $\{\chi_\mu^\alpha(\vec{r})\}$ (augmenting it by a few fixed Slater orbitals, if necessary) and the superposition potential $V_{\text{SRC}}^{\text{sup}}(\vec{r})$, $V_{\text{LRC}}^{\text{sup}}(\vec{r})$ [Eqs. (13a) and (13b)] for an assumed set $\{f_{n,i}^\alpha, Q^\alpha\}$ and use the crystal density $\rho_{\text{cry}}(\vec{r})$ from the previous iteration to compute the exchange and correlation functions. The secular problem is solved at a set of points in the BZ using the methods outline in Sec. IIB for computing the matrix elements. The full overlapping superposition density is used in a tabular form with no approximations made, such as fitting to an analytical form or extracting muffin-tin averages. The new $\rho_{\text{cry}}(\vec{r})$ is then computed from Eq. (28) and a modified set of population numbers and charges are constructed. Figure 4 shows the variation in $\Delta\rho(\vec{r})$ along the

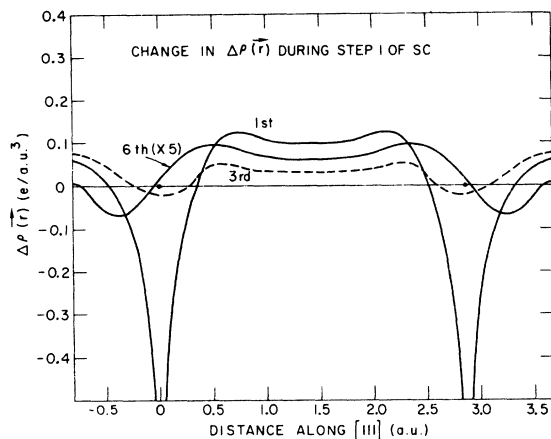


FIG. 4. Plot of $\Delta\rho(\vec{r}) = \rho_{\text{cry}}(\vec{r}) - \rho^{\text{sup}}(\vec{r})$ along the [111] direction in diamond during various steps in the charge and configuration self-consistency iterations.

[111] bond direction in diamond during CCSC iterations constructed from the six nearest-volume \vec{k} points and a minimal numerical set with the initial $1s^2 2s^2 2p^2$ configuration. The function $\Delta\rho(\vec{r})$ in the curve marked as “1st” exhibits, aside from a buildup of charge in the interatomic region (which indicate some covalent bond formation relative to the assumed superposition model), rather sharp features near the atomic sites which depict the degree to which this initial electronic configuration is inadequate in representing the output ground-state crystal density.⁶⁸ At this stage, σ [Eq. (32)] is $0.153e$ (which is to be compared with a total of 12 electrons or 8 valence electrons in the unit cell). It is obvious that to obtain a better representation of $\rho_{\text{cry}}(\vec{r})$ in terms of a superposition model one has to match better the nodes in the atomic wave functions with those of the occupied crystal functions. When only a minimal numerical set is used for diamond, the least-squares procedure reduces to handling only two degrees of freedom. If λ_1 denotes the ratio between the $2p$ to $2s$ population (“atomic hybridization ratio”) and by λ_2 the $1s$ population, then the general configuration becomes $1s^{\lambda_2} 2s^{(6-\lambda_2)/(1+\lambda_1)} 2p^{\lambda_2(6-\lambda_1)/(1+\lambda_1)}$. The λ_2 population did not vary from the value of 2.000 during iterations (since the lowest crystal wave function is given to a good approximation as a nonoverlapping sum of the undistorted atomic $1s$ orbitals) so in practice the configuration $1s^2 2s^{4/(1+\lambda_1)} 2p^{4\lambda_1/(1+\lambda_1)}$ had to be treated. A free minimization of $\sigma(\lambda_i)$ (varying the basis set at *each* iteration) yields the residual $\Delta\rho(\vec{r})$ shown in Fig. 4 as “6th” and the values $\sigma_{\text{min}} = 0.098e$ for the configuration $\lambda_1 = 1.701$, $\lambda_2 = 2.000$; $\Delta\rho(\vec{r})$ obtained at this stage exhibits some covalent bond formation in the interatomic region

along with a structure near the nuclei due to interpenetration of charges from neighboring atomic sites. This value of σ_{\min} and the deviations of the residual $\Delta\rho(\vec{r})$ from zero probably indicate the "best" level of SC attainable within a superposition model (CCSC) of a minimal numeric set.

Although the minimal value of σ at the convergence limit of CCSC is still quite large, it is remarkable that $\Delta\rho(\vec{r})$ becomes a rather smooth spatial function. Thus, while one can effectively account for all the "bonding" effects that are describable by *intra-atomic* charge redistribution in a linear superposition overlapping densities model, the *inter-atomic* rearrangement of charge remains largely undescribable by a simple superposition of (nonlinearly varied) spherical atomic densities. In systems in which ground-state charge redistribution effects are very small, one might expect to do rather well with a one-center superposition model, in which case, the results of CCSC are presumably already very close to FSC results. For example, when a minimal numerical basis set calculation is done for solid neon in the usual $1s^2 2s^2 2p^6$ configuration [lattice constant of 4.52 Å, 2000 integration points and neglecting the correlation functional in Eqs. (3) and (6)] the first iteration already produces a σ value as low as $0.003e$ (compared with a total of 10 electrons per cell) and no further changes are observed during successive iterations. On the other hand, however, for strongly covalent systems like diamond CCSC alone is not satisfactory and one should also incorporate the residual $\Delta\rho(\vec{r})$ in a more complete treatment. Before proceeding to the next stage

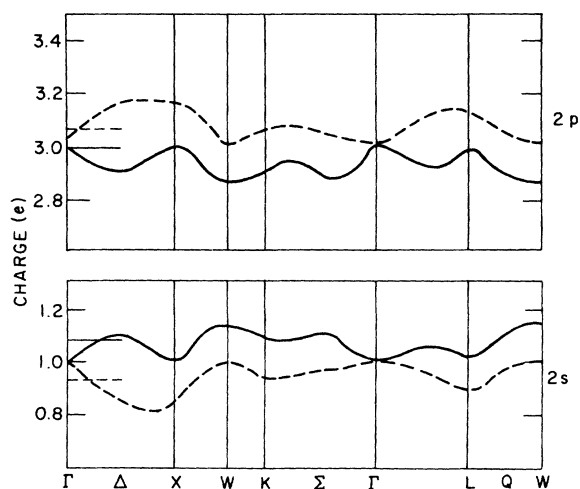


FIG. 5. Dispersion of the Mulliken (full lines) and Löwdin (dashed lines) $2s$ and $2p$ charges in diamond across the Brillouin zone. Upper figure: $2p$ charges. Lower figure: $2s$ charges. The $1s$ charge, not shown in the figure, has a dispersion of less than $10^{-2}e$ around $2.0e$

in SC, some illustrative examples of the possible arbitrariness in stage 1 need to be discussed.

A rather popular choice for a superposition model to be used in a CCSC procedure is one based on identifying the expansion coefficients a_i in Eq. (29) with either Mulliken or Löwdin atomic charge populations.^{59,60} One constructs at each iteration step a new set of populations along with the resulting superposition density and repeats the process until the populations obtained in successive iterations agree to within a prescribed tolerance. The degree to which the final $\rho_0(\vec{r})$ simulates the charge density derived directly from the wave functions remains unspecified throughout the calculation. It is thus not surprising that in previous investigations in molecular systems, different prescriptions (e.g., Mulliken or Löwdin) for partitioning the charge density into sums of atomic densities were found to lead to different convergence limits, as indicated by wildly different dipole moments, eigenvalues, etc.^{60a} It is still of some interest to find whether one can effectively approach the limit of a free minimization of σ [Eq. (32)] by using one of the commonly accepted population analysis techniques.

We have performed two independent CCSC calculations for diamond using Mulliken and Löwdin population analysis with a minimal numeric basis set, 3000 integration points, and carrying all lattice sums to eight shells of atomic neighbors. The Mulliken population⁶⁵ amounts to arbitrarily dividing equally between the relevant sites all the cross terms in the charge-density expression between basis functions located on different inequivalent sites. In the Löwdin procedure⁶⁶ one orthogonalizes the Bloch function basis first. In this case the populations are defined to be proportional to the squares of the transformed expansion coefficients. The Mulliken and Löwdin populations are calculated at a set of points in the BZ and averaged to yield the total ground-state population of each of the $1s$, $2s$, and $2p$ orbitals in the crystal. To illustrate the type and range of possible errors made by sampling only a few points in the BZ, we plot on an enlarged scale in Fig. 5 the dispersion of the Mulliken and Löwdin charges throughout the zone,

TABLE I. Brillouin-zone averages of the orbital charges in diamond (Löwdin's definition).

| Orbital | $4-\vec{k}$ | $6-\vec{k}$ | $10-\vec{k}$ | $19-\vec{k}$ | Exact |
|---------|-------------|-------------|--------------|--------------|--------|
| $1s$ | 1.9910 | 1.9792 | 1.9793 | 1.9793 | 1.9801 |
| $2s$ | 0.9452 | 0.9427 | 0.9426 | 0.9425 | 0.9420 |
| $2p$ | 3.0638 | 3.0781 | 3.0782 | 3.0782 | 3.0779 |

TABLE II. Comparison between some calculated properties obtained in three different CCSC models. Mulliken SC and Löwdin SC refer to iterative calculations based on the Mulliken and Löwdin charges, respectively; "free minimization" refers to an iterative least-squares minimization of the charge deviation σ . Energies are given in eV and populations in electron units. Eigenvalues are given with reference to the $\Gamma_{1,v}$ point at the bottom of the valence band.

| Property | Mulliken SC | Löwdin SC | Free minimization |
|--------------------------|-------------|-----------|-------------------|
| Final deviation σ | 0.1595 | 0.1714 | 0.098 |
| Eigenvalues | | | |
| $\Gamma_{25,v}$ | 20.419 | 20.426 | 20.403 |
| $\Gamma_{15,c}$ | 26.819 | 26.838 | 26.776 |
| $\Gamma_{2,c}$ | 34.547 | 34.562 | 34.530 |
| $L_{2,v}$ | 5.268 | 5.282 | 5.264 |
| $L_{3,v}$ | 17.635 | 17.648 | 17.624 |
| $L_{3,c}$ | 30.800 | 30.819 | 30.767 |
| $X_{1,v}$ | 8.276 | 8.276 | 8.269 |
| $X_{4,v}$ | 14.350 | 14.362 | 14.329 |
| $X_{1,c}$ | 29.127 | 29.138 | 29.086 |
| $X_{4,c}$ | 37.222 | 37.184 | 37.179 |
| Hybridization | | | |
| Ratio ($2p/2s$) | 2.773 | 3.265 | 1.701 |
| Total energy | | | |
| per atom (eV) | -1013.113 | -1011.235 | -1013.3990 |
| Form factors | | | |
| f_{111} | 3.206 | 3.201 | 3.210 |
| f_{222} | 0.1140 | 0.1110 | 0.1170 |
| f_{220} | 1.986 | 1.975 | 1.990 |

as computed at 24 points in the $\frac{1}{48}$ irreducible BZ section. It is seen that the charge dispersion is quite low (typically of the order of $0.15e$ for both $2s$ and $2p$ states), and that the Löwdin $2s(2p)$ charge is systematically lower (higher) than the corresponding Mulliken charges. The dispersion of the $1s$ charges in both schemes is smaller than 1 part in 10^2 and is not shown in Fig. 5. Table I shows the BZ averaged charges, using 4, 6, 10, and 19 nearest-volume points in the irreducible BZ section. It is seen that the $6-\vec{k}$ sampling produces charges that are accurate to within $0.005e$. At the end of each iteration, $\rho_0(\vec{r})$ is used to construct a new potential, and the iteration cycle is repeated until SC in populations is better than $0.005e$. A nonlinear variation of the basis set is performed at each iteration. A simple damping technique of the iteration cycle^{60c} (with a damping coefficient of 0.3) combined with the use of the "Pratt improvement scheme"⁷⁰ near convergence enables self-consistency to be obtained typically in three to six iterations. The final wave functions are used to compute the total energy per atom and the x ray form factors (Appendix A).

Table II summarizes the results obtained at a

convergence limit of these two calculations, along with those obtained in a calculation in which the arbitrary f_{1s} , f_{2s} , and f_{2p} populations were varied iteratively so as to minimize the deviation σ between $\rho_0(\vec{r})$ and $\rho_{\text{crr}}(\vec{r})$. It is evident that although the internal consistency in the populations is constrained to be good, the Löwdin and Mulliken population schemes tend to converge the result to distinctly different limits. Whereas the band structure obtained from the Mulliken schemes agrees with that obtained by the Löwdin scheme to within 0.01–0.04 eV over the valence and first conduction bands, the wave-function-dependent quantities like charges and total energy are markedly different. The difference in the Fourier-transformed total density (form factors) are quite low, while the difference in the individual orbital densities (as reflected by the $2p$ - $2s$ hybridization ratio) and total energies (which depend on higher orders of the charge density) are substantial. It is also to be noted that although neither the Löwdin nor the Mulliken schemes seem to reduce substantially $\Delta\rho(\vec{r})$ towards the limit obtained in the exact CCSC procedure ("full minimization"), the Mulliken prescription does a little better than the Löwdin scheme. It is expected that in heteropolar systems, where the difference in the charges obtained by the various definitions is much larger,^{60a} the observables calculated from the first-order density matrices within these schemes would differ even more than in diamond. Although σ_{Mull} seems to offer only a small improvement over $\sigma_{\text{Löwd}}$, properties that are sensitive to the details of the charge density (e.g., those nonlinear in the density like the total energy) can come out substantially different. Thus, due to the fact that the Mulliken $\Delta\rho(\vec{r})$ happened to be much smoother near the core regions than the Löwdin $\Delta\rho(\vec{r})$ (although they are rather similar in the valence region), the total energy obtained in the former procedure is closer to that obtained in the "full minimization." By contrast, the x-ray form factors that sample mainly the interatomic region (e.g., the "forbidden" [222] reflection) are quite similar in all three calculations. Note that since the "exact" $\Delta\rho(\vec{r})$ has a null zeroth moment (by construction) and is rather smooth throughout space, the errors associated with using this superposition model would probably be distributed rather uniformly in space and not cause too severe a problem for such properties as atomic scattering factors. We conclude that although SC schemes within a superposition model can be useful in obtaining "simple" quantities such as eigenvalues, they should be treated with great care as to the behavior of the residual densities when more complicated properties are investigated. In parti-

TABLE III. Comparison of basis-set effects in different non-self-consistent calculations in diamond with exchange coefficient $\alpha = 1$ and a lattice constant $a = 6.728$ a.u. Energies are given in eV. The number of plane waves (PW) or atomic orbitals used in each case, is indicated.

| Level | OPW ^a 90-PW | OPW ^b 331-PW | LCAO ^c 20 Slater orbitals | LCBO ^d 10 Slater orbitals | Present work ^e minimal set | Present work ^f extended set |
|-----------------|---------------------------|----------------------------|--|--|--|---|
| Γ_{1v} | 0.0 | 0.0 | 0.0 | 0.0 | 0.0 | 0.0 |
| Γ_{25v} | 22.97 | 22.3 | 20.22 | 20.15 | 20.47 | 20.12 |
| Γ_{15c} | 28.60 | 28.8 | 26.45 | ... | 27.65 | 27.33 |
| $\Gamma_{2',c}$ | 36.57 | 34.3 | 33.58 | ... | 33.52 | 33.42 |
| $L_{2',v}$ | 5.80 | 5.5 | 5.17 | 5.39 | 5.19 | 5.19 |
| $L_{1,v}$ | 8.52 | 8.9 | 7.92 | 8.66 | 8.41 | 8.39 |
| $L_{3',v}$ | 17.69 | 19.7 | 17.50 | 17.56 | 17.76 | 17.74 |
| $L_{3',c}$ | 27.91 | 31.7 | 30.23 | ... | 30.28 | 30.20 |
| L_{1c} | 31.27 | 30.4 | 30.23 | ... | 30.31 | 30.28 |
| L_{2c} | ... | 39.7 | 37.98 | ... | 37.62 | 37.51 |
| $X_{1',v}$ | 8.86 | 8.8 | 8.08 | 8.49 | 8.26 | 8.26 |
| X_{4v} | 15.84 | 16.2 | 14.58 | 14.59 | 14.51 | 14.49 |
| X_{1c} | 27.10 | 27.4 | 28.27 | ... | 28.38 | 28.31 |
| X_{4c} | ... | 41.1 | 36.46 | ... | 36.84 | 36.72 |

^aReference (3).

^bReference (73).

^cReference (11).

^dReference (12a).

^eMinimal numeric set of $1s$, $2s$, and $2p$.

^fSame as e plus $3s$, $3p$, and $3d$ Slater orbitals.

cular, when $\Delta\rho(\vec{r})$ is non-negligible the SC cycle can converge to an arbitrary limit.⁷¹

C. Full self-consistency

The procedure used to obtain FSC is based on the properties of the residual density $\Delta\rho(\vec{r})$ as obtained at the convergence limit of the CCS, namely: (i) $\Delta\rho(\vec{r})$ is constructed to integrate exactly to zero over the unit-cell volume; (ii) it has a rather small numerical value over the unit cell space due to the use of a least-squares minimization in the CCSC; (iii) It is a rather *smooth* function of space. More specifically, both the characteristic cusps at the position of the nuclei and the steep variation near the core regions characterizing the full charge density [and the unoptimized $\Delta\rho(\vec{r})$] are completely eliminated by carrying stage 1 in SC successfully to convergence. (iv) It has the full symmetry of the crystal. These properties suggest that $\Delta\rho(\vec{r})$ would lend itself to a rapidly convergent Fourier-series representation.

Fourier components of $\Delta\rho(\vec{r})$ are determined for a list of RLV (\vec{K}_s 's) shorter than some prescribed length, using a direct three-dimensional integration over the unit cell (uc):

$$\Delta\rho(\vec{K}_s) = \frac{1}{\Omega} \int_{uc} e^{-i\vec{K}_s \cdot \vec{r}} \Delta\rho(\vec{r}) d\vec{r}. \quad (33)$$

They are employed to construct the iterated correction to the electronic Coulomb potential,

$$\Delta V_{Coul}(\vec{r}) = \sum_{\vec{K}_s \neq 0} -4\pi \frac{\Delta\rho(\vec{K}_s)}{K_s^2} e^{i\vec{K}_s \cdot \vec{r}}. \quad (34)$$

The sum over the RLV is expected to converge rapidly due both to the smooth form of $\Delta\rho(\vec{r})$ and to the K_s^{-2} factor. The exchange and correlation potentials used in the iteration cycle are simply constructed in *real space* using the full density $\rho_{crr}(\vec{r})$ and the functional in Eqs. (6) and (7) thus avoiding the difficulties encountered in Fourier expanding these nonlinear functions.^{50,51} The solution to the band problem is now repeated with the refined potential using the fixed numerical basis set and $V_{SRC}^{sup} + V_{LRC}^{sup}(\vec{r})$ obtained in the last step of the CCSC. The resulting crystal eigenfunctions are used to construct a refined crystal density via Eq. (28) and a new $\Delta\rho(\vec{r})$ and $\Delta\rho(\vec{K}_s)$. The calculation is repeated iteratively until the relative change in the most sensitive Fourier components between successive iterations is lower than 10^{-5} . If stage 1 in SC is carried properly to convergence, only a few iterations (two to six in diamond) are required in stage 2 and only the first few stars of the RLV (five to ten in diamond) are required. The $\Delta\rho(\vec{K}_s)$ values for large \vec{K}_s reflect the core contribution to $\Delta\rho(\vec{r})$ and are, hence, negligibly small since they have been absorbed in $\rho_0(\vec{r})$ in the CCSC stage.

V. ENERGY-BAND STUDIES

A. Basis-set convergence

Although a meaningful study of basis-set effects in a variational theory should be based preferably on considerations of the total energy, none of the

previously published calculations have attempted such a task. Thus, we are forced to refer mainly to the resulting eigenvalues and use the total energy only as an internal criterion for examining the quality of our various basis functions. Since previously published LCAO studies on diamond were not carried out to SC nor calculated with the correlation functional [Eq. (7)], we will make comparisons with our calculations obtained at this level of approximation. Whenever a different lattice constant or exchange parameter was used in the literature, we have repeated our calculation to match these values as closely as possible. Since one object of this particular study is to compare the accuracy of various basis sets in realistic *ab initio* studies, no reference is made to empirical pseudopotential results, empirical tight binding, empirically adjusted *ab initio* results or muffin-tin calculations.

Among the previously published *ab initio* LDF models for diamond in the LCAO representation we refer to the Slater basis set calculation of Chaney, Lin, and Lafon,¹¹ the discrete variational study of Painter, Ellis, and Lubinsky,⁸ the Gaussian basis calculation of Simmons *et al.*,¹³ and the linear-combination of bond orbitals (LCBO) of Kervin and Lafon.^{12a} Several first-principles OPW studies have been made in the past on diamond, e.g., the plane-wave calculation of Herman⁷² and Bassani and Yoshimine,³ the 302–331 plane-wave calculation of Rudge⁷³ and the 965 plane-wave study of Euwema and Stukel.⁵ These calculations are non-self-consistent, and slightly different *ad hoc* potentials have been assumed by the various authors.⁷⁴

Table III compares our results with energy eigenvalues of the four valence and two lowest conduction bands at the high-symmetry points, Γ , X , and L in diamond obtained by various OPW and LCAO methods with an exchange coefficient of 1.0 ("Slater exchange") and a lattice constant of 6.728 a.u. Our non-self-consistent results are presented using a minimal numerical basis set of 1s, 2s, and 2p orbitals and the extended set in which 3s, 3p Slater-type orbitals (with exponents of 1.4 and 2.64, respectively) were added. In the states that contain no p character the internal consistency between the various OPW studies is about ~ 1 eV and a similar agreement is obtained with our minimal basis-set calculations. For states that contain p character, our results are some 2–3 eV lower than the best OPW result signaling serious convergence errors in the OPW results.⁷⁵

Our *minimal numerical basis-set* results and the minimal LCAO basis-set results of Chaney *et al.*¹¹ (and Kervin and Lafon^{12a}) agree to within 0.15 eV/state (i.e., a simple average on the four va-

lence and two conduction bands at the Γ , X , and L points), and to within 0.10 eV/state for their extended basis set. Part of the remaining discrepancy can well be due to the linearization of the exchange functional in the LCAO studies¹² and to the slightly different superposition potentials used.

Our extended basis set produces eigenvalues that are on the average 0.05 eV lower than those obtained with the minimal numerical set. We have studied a series of extended basis sets, augmenting the minimal set by *numerical* 3s, 3p, and 3d states and various Slater-type 3d and 3p states. (In neither case do the eigenvalues presented in Table III change by more than an average of 0.07 eV relative to the minimal numerical set results.) We thus conclude that a minimal numerical set produces eigenvalues for the valence and lowest two conduction bands that are roughly equivalent to those obtained by an extended analytical Slater set. As a further check, we have compared these eigenvalues to those obtained by Painter *et al.*⁸ with a double-zeta set, a lattice constant of 6.720 a.u. and an exchange parameter $\alpha = 0.758$ ("Schwarz value"⁷⁶). Since only a few of their eigenvalues are quoted in their paper, we repeated their calculation with their Slater basis set and parameters. These results are compared in Table IV with our minimal and extended basis-set results. The agreement with our minimal numeric set is again 0.10 eV/state on the average, our (relative) eigenvalues lying consistently *below* those obtained with the double-zeta set.

In a comparative study, Painter *et al.*⁸ have

TABLE IV. Comparison of basis-set effects between various LCAO expansion sets. $\alpha = 0.75829$; $a = 6.720$ a.u. Energy in eV.

| Level | LCAO | | |
|-----------------|--------------------|------------------------------|---------------------------|
| | 18 Slater orbitals | Present work minimal numeric | Present work extended set |
| $\Gamma_{1,v}$ | 0.0 | 0.0 | 0.0 |
| $\Gamma_{25,v}$ | 20.89 | 20.47 | 20.38 |
| $\Gamma_{15,c}$ | 26.83 | 26.54 | 26.45 |
| $\Gamma_{2',c}$ | 35.24 | 34.76 | 34.68 |
| $L_{2',v}$ | 5.65 | 5.35 | 5.34 |
| $L_{1,v}$ | 7.38 | 7.21 | 7.20 |
| $L_{3',v}$ | 17.91 | 17.68 | 17.65 |
| $L_{3',c}$ | 30.75 | 30.41 | 30.38 |
| $L_{1,c}$ | 31.81 | 31.17 | 31.15 |
| $L_{2',c}$ | 38.79 | 38.15 | 38.09 |
| $X_{1,v}$ | 8.33 | 8.32 | 8.31 |
| $X_{4,v}$ | 14.36 | 14.36 | 14.32 |
| $X_{1,c}$ | 28.51 | 28.21 | 28.20 |
| $L_{4,c}$ | 37.87 | 37.34 | 37.30 |

used their double-zeta Slater basis set to compute the band structure of diamond using the muffin-tin potential previously employed by Keown in his highly converged APW study.⁶ Painter *et al.* found an average agreement of ~ 0.05 eV/state with the "exact" muffin-tin results, their values being usually *above* the APW results. This tends to indicate that our minimal basis set results are as good as, or slightly better than, the APW results and of roughly the same quality as an extended Slater basis set. We believe our extended set to be superior to all other basis sets discussed.

In order to study the variational quality of some of the basis sets employed, we have calculated the total ground-state energy per atom using the experimental lattice constant⁷⁷ of 6.7403 a.u. and $\alpha = \frac{2}{3}$ (neglecting correlation) (see Appendix A for a description of the total energy-calculation scheme). The results are presented in Table V along with those obtained by augmenting a minimal numerical set with two sets of identical sizes, corresponding to positively and negatively charged carbon atoms (consisting of a charge-transfer ion-pair basis set).⁷⁸

A further test of the variational quality of the LCAO basis set was performed by examining truncated analytical orbitals. It has been previously suggested¹³ that one may significantly reduce the computational effort associated with performing lattice sums over the rather long-range atom-like analytical orbitals with little loss in the accuracy of the eigenvalues, by projecting out these long-range tails. Following Simmons *et al.*¹³ we have curve fitted the $3s$ and $3p$ Slater orbitals with several short-range Slater orbitals, and have discarded the long-range components. The resulting $3s$ and $3p$ orbitals were then virtually iden-

tical to the original ones up to a distance of 1.8 a.u. from the nucleus and then decayed almost twice as fast as the original orbitals. The results for this basis set are shown in the last line of Table V.

The following conclusions may be drawn from this study:

(i) Augmenting the minimal numerical set by $3s$ - and $3p$ -type orbitals has the effect of stabilizing the crystal ground-state energy by about 0.9–1.1 eV/atom. This stabilization is similar for both atomic (untruncated) Slater-type or numerical orbitals. The addition of these orbitals changes the valence-band eigenvalue spectrum only an average of by 0.02 eV/state. The details of the two lowest conduction bands are changed on the average by as much as 0.06 eV/state. Hence, even a rather small mixing of the virtual atomic states into the occupied manifold in the solid, produces a substantial total energy stabilization, although the accompanying change in the eigenvalues is small.

(ii) A very significant lowering of the total energy, by 2.5 eV/atom, is produced by adding the ion-pair basis set to the initial minimal numerical set. Again, the average change in the eigenvalues is rather small (0.03 eV/state in the valence bands and 0.05 eV/state in the two lowest conduction bands). Examination of the crystal density shows that the ion-pair basis set changes only negligibly the charge in the interatomic bonding region and that the substantial penetration of the ion-pair orbitals into the core region of the neighboring sites is responsible for most of the variational stabilization. We were unable as yet to optimize the total energy as a function of the assumed ionicity of the ion-pair set, due to the substantial cost of such calculations. We have instead performed the calculation using three discrete values for the ionicity, namely $\pm 0.50e$, $\pm 0.80e$, and $\pm 1.00e$. The results indicate that the choice of $\pm 0.80e$ for the ionicity (a "best" value of $\pm 0.85e$ was obtained by interpolation) produces the best total energy, while the results obtained with a choice of $\pm 0.50e$ are poorer by 0.25 eV/atom. The results obtained for the choice of $\pm 1.0e$ are substantially worse than those obtained with no ion-pair set (this is probably due to the high interelectronic repulsion in the neighboring core region caused by the tails of the $Q = \pm 1.0e$ basis functions).

(iii) The use of truncated Slater orbitals along with the minimal numeric set introduces a serious destabilization of the system so that over 60% of the improvement in energy offered by the Slater orbitals is lost. This result is probably quite sensitive to the exact form of the truncation pro-

TABLE V. Total ground-state energies per atom (in eV) for diamond as obtained in a non-self-consistent calculation, for various choices of basis sets. An exchange parameter of $\frac{2}{3}$ was used and a lattice constant of 6.7403 a.u. Correlation is omitted throughout and 6 \vec{k} points are used to sample the charge density in the BZ.

| Basis set | Total energy |
|-------------------------------------|--------------|
| Minimal numerical ^a | -1012.728 |
| Extended set I ^b | -1013.418 |
| Extended set II ^c | -1013.792 |
| Ion-pair ^d | -1015.218 |
| Chopped extended set I ^e | -1013.028 |

^a $1s, 2s, 2p$ numerical local density orbitals.

^b Set a plus Slater orbitals $3s, 3p$ (see text).

^c Set a plus numerical $3s, 3p$ orbitals.

^d Set a plus two comparable sets for a positively and a negatively charged carbon atoms (see text).

^e Set a plus truncated $3s, 3p$ Slater orbitals.

cedure and no general statement can be made about the "optimum" truncation without extensive experimentation. It seems, however, that the relative insensitivity of the band structure to a particular truncation (0.09 eV/state on the average, in our case) could hardly be used as an indication of its adequacy, especially in covalently bonded systems in which penetration of the tails coming from neighboring atoms into the core region of the central atom contribute significantly to the stability of the system.

B. Convergence of reciprocal and direct lattice sums

As stated in Sec. IV, we use a special \vec{k} -point algorithm^{56,57} to calculate the iterated crystal density [Eq. (28)]. Several objections have been raised recently as to the adequacy of a small \vec{k} sampling set in SC band calculations.^{50,55} Naturally, the key problem in obtaining a good BZ average of a wave-vector-dependent property is its degree of dispersion. Figure 5 showed that the Mulliken and Löwdin orbital populations derived from the charge density have a remarkably low dispersion even in a wide-band material like diamond. Table I shows the BZ average of these orbital charges as calculated by the 4, 6, 10, and 19 special \vec{k} points used in our SC cycle to determine the crystal density, together with an accurate determination of those quantities calculated by using a numerical integration of the orbital charge dispersion curves of Fig. 5. It is seen that a 6- \vec{k} -point integration scheme is already capable of producing extremely accurate results for these averages. Figure 6 shows the total ground-state

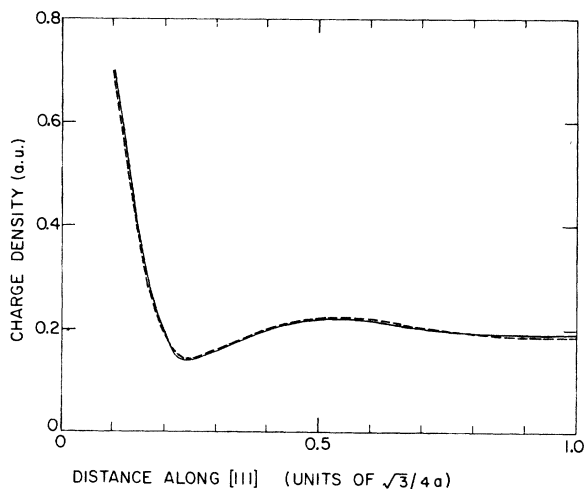


FIG. 6. Average of the valence charge along the [111] direction in diamond; full line: 6-nearest-volume \vec{k} points; dashed lines: 10-nearest-volume \vec{k} points. The results for 19-nearest-volume \vec{k} points are indistinguishable from the 10-points density, on this scale.

charge density along the bonding [111] direction as calculated by the 6- \vec{k} averaging schemes. The 19- \vec{k} scheme produced results that are indistinguishable from the 10- \vec{k} results on the scale of Fig. 6. It is to be noted that although the band-by-band charge density shows non-negligible dispersion, the total ground-state density of the closed-shell system is quite constant throughout the BZ. We also note that the BZ averages of the *band eigenvalues* needed for the total energy calculation (Appendix A) cannot be estimated accurately by a special \vec{k} -point algorithm (with a few sampling points, as used for the charge density) due to the substantial width of the occupied bands in diamond, and that this quantity is calculated by numerically integrating the occupied part of the one-electron band structure (Appendix A).

In examining the effect of the BZ sampling scheme on the calculated x-ray scattering factors, the results of the 4-, 6-, and 19- \vec{k} -point samplings (Table VI) demonstrate the small dispersion of the Fourier-transformed charge density throughout the BZ. However, we have found⁷⁹ that in *heteropolar* III-V compounds such as boron nitride, where hybridization between the orbitals of the different atoms in the unit cell is important, the charge density exhibits much larger variations in the BZ due to the change of hybridization ratio and degree of interatomic charge transfer with the symmetry of the state in the zone. In such cases, BZ averages needed for the SC cycle should be done with more sampling points.

Since space lattice sums are encountered in constructing the superposition charge density [Eq. (10)], the short-range potential [Eq. (13a)] and the basis Bloch functions [Eq. (16)], we have examined the convergence of various calculated properties. When only a minimal numeric basis set was used, a cutoff distance of 14 a.u. produced energy bands that are stable to within 0.15 eV towards any further increase in the summation range, while inclusion of long-range virtual (numerical) orbitals necessitates a much longer range. We have found, however, that if one obtains these orbitals from the solution of Eq. (19) with a localizing potential $A(r)$ in the form of an external potential well,^{45,46}

TABLE VI. Brillouin-zone averages of the x-ray scattering factors in diamond, as obtained by different \vec{k} -point sampling schemes.

| hkl | 4 \vec{k} | 6 \vec{k} | 19 \vec{k} |
|-------|-------------|-------------|--------------|
| 111 | 3.281 | 3.273 | 3.271 |
| 220 | 1.995 | 1.992 | 1.990 |
| 311 | 1.692 | 1.720 | 1.720 |
| 222 | 0.139 | 0.137 | 0.135 |

it is possible to reduce the long-range character of these orbitals without any significant loss in the accuracy of the resulting eigenvalues and total energy. The distance from the atomic origin at which this well was constructed was fixed by the requirement that this external potential will not change the spatial behavior of the low-lying core plus valence atomic orbitals. With this choice, it was possible to converge the lattice sums of the Bloch orbitals [Eq. (16)] by using a cutoff distance of 18 a.u.; an accurate total-energy evaluation required a larger cutoff distance of about 23 a.u. It thus seems that the numerical basis set in this work offers a natural and convenient way of localizing the long-range free space atomic orbitals, thereby avoiding the difficulties associated with slowly convergent lattice sums.^{13,31,32}

VI. SUMMARY

We have presented a combined Fourier-transform and discrete variational approach to the problem of obtaining self-consistent solutions to the local-density one-particle equations for solids. The method is based on systematic extensions of non-self-consistent real-space techniques of Ellis, Painter, and co-workers^{8,9} as well as SC reciprocal space methodologies of Chaney, Lin, Lafon, and co-workers.¹¹⁻¹³ Our method overcomes the usual difficulties in "standard" APW or Korringa-Kohn-Rostoker techniques by avoiding completely the muffin-tin approximation to the potential and charge density and greatly simplifies the problems of basis-set convergence encountered in tight-binding Gaussian expansion techniques. Complete self-consistency is conveniently obtained by combining the treatment of the iterated superposition potential (with its large nonconstant spatial terms in a real-space numerical integration approach) with a Fourier decomposition and reciprocal space sums of the smooth charge-density difference that are not amenable to a CCSC analysis. All the many-center integrations appearing in standard tight-binding approaches are avoided by the use of a direct Diophantine numerical integration scheme. We believe that with the use of an efficient numerical basis and the techniques outlined above for obtaining self-consistent solutions, we have come quite close to

the point where the predictions of the local density formalism for real solids can be critically compared with other theoretical approaches to the electronic structure problem.

ACKNOWLEDGMENTS

We are grateful to D. E. Ellis for making available his non-self-consistent DVM program and for helpful collaboration during an early phase of this work. We thank F. Averill, R. N. Euwema, J. L. Calais, and A. Seth for stimulating discussions.

APPENDIX A: CALCULATION OF OBSERVABLES

The wave functions, charge density, and potential are used at the end of the SC cycles to compute the total ground-state energy and the x-ray scattering factors. We outline here briefly the computational schemes used to calculate these observables.

1. *Total energy.* The total ground-state energy is computed for a fixed set of nuclear coordinates and lattice vectors from Eq. (4). Using the fact that the band eigenvectors $\psi_j(\vec{k}, \vec{r})$ are solutions of our one-particle equation, the kinetic energy is given by

$$E_{KE} = \sum_{j, \vec{k}} \epsilon_j(\vec{k}) - \int \rho_{\text{crr}}(\vec{r}) [V_{ne}(\vec{r}) + V_{ee}(\vec{r}) + \frac{4}{3}V_x(\vec{r}) + V_{\text{corr}}(\vec{r})] d\vec{r}, \quad (\text{A1})$$

where the various potential terms are

$$V_{ne}(\vec{r}) = \sum_m \frac{Z_m}{|\vec{r} - \vec{R}_m|}, \quad (\text{A2})$$

$$V_{ee}(\vec{r}) = \int \frac{\rho(\vec{r}')}{|\vec{r} - \vec{r}'|} d\vec{r}',$$

and $V_x(\vec{r})$ and $V_{\text{corr}}(\vec{r})$ are given by Eqs. (6) and (7). The total potential energy is given by

$$E_{PE} = \int \rho_{\text{crr}}(\vec{r}) [V_{ne}(\vec{r}) + \frac{1}{2}V_{ee}(\vec{r}) + V_x(\vec{r}) + V_{\text{corr}}(\vec{r})] d\vec{r}_{+V_{nn}}, \quad (\text{A3})$$

where V_{nn} is the internuclear repulsion term. Since V_{en}/N , V_{ee}/N , and V_{nn}/N are divergent as N goes to infinity, we rearrange the terms in the potential energy to yield

$$E_{PE} = \frac{1}{2} \int \rho_{\text{crr}}(\vec{r}) [V_{ne}(\vec{r}) + V_{ee}(\vec{r})] d\vec{r} + \left(\frac{1}{2} \int \rho_{\text{crr}}(\vec{r}) V_{ne}(\vec{r}) d\vec{r} + V_{nn} \right) + \int \rho_{\text{crr}}(\vec{r}) [V_x(\vec{r}) + V_{\text{corr}}(\vec{r})] d\vec{r}. \quad (\text{A4})$$

In this form, the divergences in the individual terms are grouped to yield the three finite terms in (A4), each linear in N , so that a total energy per unit cell can be defined. The first two terms in (A4) represent the total electrostatic energy while the last term is the total exchange and correlation energy. When the total electrostatic energy in Eq. (A4) is rearranged, one obtains the expression

$$E_{\text{elec}} = \frac{1}{2} \int \rho_{\text{cry}}(\vec{r}) [V_{ne}(\vec{r}) + V_{ee}(\vec{r})] d\vec{r} + \frac{1}{2} \sum_{\alpha=1}^h Z_{\alpha} [V_{\text{vac}}(\alpha) + V_{ee}(\alpha)], \quad (\text{A5})$$

where the "vacancy potential" $V_{\text{vac}}(\alpha)$ is defined as the total electrostatic potential at the α th site due to all charges except those of the α th site itself, and $V_{ee}(\alpha)$ is the value of the electronic potential energy at this site. To calculate the total energy we thus need to perform three integrals over the unit cell volume, namely, over $\rho_{\text{cry}}(\vec{r}) [V_{ne}(\vec{r}) + V_{ee}(\vec{r})]$, $\rho_{\text{cry}}(\vec{r}) V_x(\vec{r})$, and $\rho_{\text{cry}}(\vec{r}) V_{\text{corr}}(\vec{r})$ and two sums [in Eqs. (A1) and (A5)]. The exchange and correlation integrals were found to converge readily using about 2000 Diophantine sample points, while the Coulomb integration was found to converge more slowly. The terms $\rho_{\text{cry}}(\vec{r}) V_{ne}(\vec{r})$ and $\rho_{\text{cry}}(\vec{r}) V_{ee}(\vec{r})$ are combined before integration is attempted. It was found, however, that no further simplifications of the Coulomb integral are required in order to obtain good accuracy in its evaluation; about 4000–7000 integration points, combined with a highly peaked sample point distribution in the core region, were sufficient to obtain good accuracy in the cohesive energy.

The sum over the band eigenvalues in Eq. (A1) was performed using 32 equally spaced points in the

$\frac{1}{48}$ irreducible BZ section. Sufficient accuracy in the crystal core eigenvalues is assured by employing some 10–30 integration points inside the nuclear volume and about 300 points within the 1s orbital sphere.

The total energy of the free atom is computed from a spin-polarized version of the Herman-Skillman program using the correlation functional from Eq. (7).

2. *X-ray scattering factors.* The x-ray scattering factors $f(\vec{K})$ are computed from the SC $\rho_{\text{cry}}(\vec{r})$ by a direct three-dimensional Diophantine integration

$$f(\vec{K}) = \frac{1}{\Omega} \int e^{i\vec{K}\cdot\vec{r}} \rho_{\text{cry}}(\vec{r}) d\vec{r} \quad (\text{A6})$$

for a set of (h, k, l) reflections \vec{K} . Although the convergence of this integral as a function of the number of sampling points is rather good (0.2% error for 2000 points in diamond), it was found somewhat advantageous to combine a radial (one dimensional) integration of the spherical components of $\rho_0(\vec{r})$ [Eq. (31)] with a Diophantine integration of $[\rho_{\text{cry}}(\vec{r}) - \rho_0(\vec{r})]e^{i\vec{K}\cdot\vec{r}}$.

*Supported by the NSF (DMR Grant No. 72-03101 and 72-03019) and the AFOSR (Grant No. 76-2948).

¹P. Hohenberg and W. Kohn, Phys. Rev. B 136, 864 (1964).

²W. Kohn and L. J. Sham, Phys. Rev. A 140, 1133 (1965).

³F. Bassani and M. Yoshimine, Phys. Rev. 130, 20 (1963).

⁴L. Kleinman and J. C. Phillips, Phys. Rev. 125, 819 (1962).

⁵R. N. Euwema and D. J. Stukel, Phys. Rev. B 1, 4692 (1970).

⁶R. Keown, Phys. Rev. 150, 568 (1966).

⁷J. R. P. Neto and L. G. Ferreira, J. Phys. C 6, 3430 (1973).

⁸G. S. Painter, D. E. Ellis, and A. R. Lubinsky, Phys. Rev. B 4, 3610 (1971); D. E. Ellis and G. S. Painter, *ibid.* 2, 2887 (1970).

⁹A. R. Lubinsky, D. E. Ellis, and G. S. Painter, Phys. Rev. B 11, 1537 (1975).

¹⁰J. B. Danese, J. Chem. Phys. 61, 3071 (1974); J. B. Danese and J. W. D. Connolly, Int. J. Quantum. Chem. Symp. 7, 279 (1973).

¹¹R. C. Chaney, C. C. Lin, and E. E. Lafon, Phys. Rev. B 3, 459 (1971).

¹²(a) P. W. Kervin and E. E. Lafon, J. Chem. Phys. 58, 1535 (1973); (b) E. E. Lafon, MIT Solid State and Molecular Theory Group Quarterly Progress Report No.

69, p. 66 (1968) (unpublished).

¹³J. E. Simmons, C. C. Lin, D. F. Fouquet, E. E. Lafon, and R. C. Chaney, J. Phys. C 8, 1549 (1975).

¹⁴E. J. Baerends, D. E. Ellis, and P. Ros, Chem. Phys. 2, 41 (1973).

¹⁵H. Sambe and R. H. Felton, J. Chem. Phys. 62, 1122 (1975).

¹⁶C. B. Haselgrove, Math. Compt. 15, 373 (1961).

¹⁷D. E. Ellis and G. S. Painter, Phys. Rev. B 2, 7887 (1970).

¹⁸F. W. Averill, Phys. Rev. B 6, 3637 (1972).

¹⁹E. C. Snow, Phys. Rev. B 8, 5391 (1973).

²⁰J. F. Janak, V. L. Moruzzi, and A. R. Williams, Phys. Rev. B 12, 1257 (1975).

²¹M. Rasolt and D. J. W. Geldart, Phys. Rev. Lett. 35, 1234 (1975).

²²P. Nozières and D. Pines, Phys. Rev. 14, 442 (1958).

²³D. Pines, *Elementary Excitations in Solids* (Benjamin, New York, 1963).

²⁴K. S. Singwi, A. Sjölander, P. M. Tosi, and R. H. Land, Phys. Rev. B 1, 1044 (1970).

²⁵L. Hedin and B. I. Lundqvist, J. Phys. C 4, 2064 (1971).

²⁶B. Y. Tong and L. J. Sham, Phys. Rev. 144, 1 (1966).

²⁷O. Gunnarsson, P. Johansson, S. Lundqvist, and B. I. Lundqvist, Int. J. Quantum Chem. Symp. 9, 83 (1975); O. Gunnarsson and B. I. Lundqvist, Phys. Rev. B 13, 4274 (1970).

- ²⁸G. S. Painter, J. S. Faulkner, and G. M. Stocks, *Phys. Rev. B* **9**, 2448 (1974).
- ²⁹N. Elyashar and D. D. Koelling, *Phys. Rev. B* **13**, 5362 (1976).
- ³⁰A. Zunger and A. J. Freeman, *Int. J. Quantum Chem.* (to be published).
- ³¹R. N. Euwema, and D. L. Wilhite, and G. T. Surratt, *Phys. Rev.* **7**, 818 (1973).
- ³²G. T. Surratt, R. N. Euwema, and D. L. Wilhite, *Phys. Rev. B* **8**, 4019 (1973).
- ³³G. G. Wepfer, R. N. Euwema, G. T. Surratt, and D. L. Wilhite, *Phys. Rev. B* **9**, 2670 (1974).
- ³⁴R. N. Euwema and R. L. Green, *J. Chem. Phys.* **62**, 4455 (1975).
- ³⁵F. Herman and S. Skillman, *Atomic Structure Calculations* (Prentice-Hall, Englewood Cliffs, N.J., 1963).
- ³⁶P. P. Ewald, *Ann. Phys. (Leipz.)* **64**, 753 (1971).
- ³⁷M. P. Tosi, in *Solid State Physics*, edited by F. Seitz and D. Turnbull (Academic, New York, 1964), Vol. 16, p. 1.
- ³⁸K. H. Johnson and F. C. Smith, in *Computational Methods in Band Theory*, edited by P. M. Marcus, J. F. Janak, and A. R. Williams (Plenum, New York, 1971), p. 377.
- ³⁹P. D. DeCicco, *Phys. Rev.* **153**, 931 (1967).
- ⁴⁰All three-dimensional plots shown are produced by the perspective hidden-line subroutine PICTURE of M. L. Prueitt. The authors are indebted to Dr. Prueitt for supplying this routine. All plots are generated from calculated data without interpolation.
- ⁴¹W. G. Richards, T. E. Walker, and R. K. Hinkley, *A Bibliography of Ab Initio Molecular Wave Functions* (Clarendon, Oxford, 1971).
- ⁴²In other calculations (e.g., Refs. 11 and 13) the lowering of the one-electron eigenvalues (band structure) as a result of augmenting or changing a basis set was taken as a criteria for the variational superiority of the augmented set. We avoid using a criteria of this nature. Calculations on molecules (e.g., Ref. 41) and solids (e.g., Ref. 43) have demonstrated that due to the fact that the sum over eigenvalues forms only a part of the total energy (usually of kinetic nature), changes in the basis set or redistribution of the electrons among different orbitals can result in lowering of the eigenvalues and a simultaneous *destabilization* of the total energy.
- ⁴³A. Zunger, *J. Chem. Phys.* **63**, 4854 (1975).
- ⁴⁴R. Latter, *Phys. Rev.* **99**, 510 (1955).
- ⁴⁵R. E. Watson, *Phys. Rev.* **111**, 1108 (1958).
- ⁴⁶F. W. Averill and D. E. Ellis, *J. Chem. Phys.* **59**, 6412 (1973).
- ⁴⁷W. H. Adams, *J. Chem. Phys.* **34**, 89 (1961); **37**, 20009 (1967); T. L. Gilbert, in *Molecular Orbitals in Chemistry, Physics and Biology*, edited by P. O. Löwdin (Academic, New York, 1964).
- ⁴⁸P. O. Löwdin, *Int. J. Quantum Chem. Symp.* **1**, 811 (1967); *Adv. Phys.* **5**, 1 (1956).
- ⁴⁹H. J. Conroy, *J. Chem. Phys.* **47**, 5307 (1967).
- ⁵⁰D. M. Drost and J. L. Fry, *Phys. Rev. B* **5**, 684 (1972).
- ⁵¹(a) J. Callaway and J. L. Fry, in *Computational Methods in Band Theory*, edited by P. M. Marcus, J. F. Janak, and A. R. Williams (Plenum, New York, 1971), p. 512; (b) J. Callaway and C. S. Wong, *Phys. Rev. B* **7**, 1096 (1973).
- ⁵²R. C. Chaney, E. E. Lafon, and C. C. Lin, *Phys. Rev. B* **4**, 2734 (1971).
- ⁵³It is noted that this type of cancellation between kinetic and potential terms is effective only for Bloch states of the type defined in Eq. (16). The alternative form $\Psi_{\mu}^{\alpha}(\vec{k}, r) = e^{i\vec{k}\cdot\vec{r}} \sum_{n} \chi_{\mu}(\vec{r} - \vec{R}_n - \vec{d}_{\alpha})$ used by Harris and Monkhorst (Ref. 54) in which the sum of atomic orbitals is plane-wave modulated, does not provide effective cancellation since $\hat{T} \Psi_{\mu}^{\alpha}(\vec{k}, \vec{r})$ does not contain a positive (atomiclike) singularity. Using the form $\Psi_{\mu}^{\alpha}(\vec{k}, \vec{r})$ instead of Eq. (16) with a small basis set we obtained good accuracy in the virtual band energies but poor accuracy in the core states.
- ⁵⁴F. E. Harris and H. J. Monkhorst, in *Computational Methods in Band Theory*, edited by P. M. Marcus, J. F. Janak, and A. R. Williams (Plenum, New York, 1971), p. 517.
- ⁵⁵N. E. Brener, *Phys. Rev. B* **7**, 1721 (1973).
- ⁵⁶D. J. Chadi and M. L. Cohen, *Phys. Rev. B* **8**, 5747 (1973).
- ⁵⁷H. J. Monkhorst and J. D. Pack, *Phys. Rev. B* **13**, 5188 (1976).
- ⁵⁸K. H. Johnson and F. C. Smith, in *Computational Methods in Band Theory*, edited by P. M. Marcus, J. F. Janak, and A. R. Williams (Plenum, New York, 1971), p. 377.
- ⁵⁹E. J. Baerends, D. E. Ellis, and P. Ros, *Theor. Chim. Acta* **27**, 339 (1972).
- ⁶⁰(a) E. W. Stout and P. Politzer, *Theor. Chim. Acta* **12**, 379 (1968); (b) B. J. Duke, *ibid.* **9**, 760 (1968); (c) R. Rein, H. Fukuda, H. Win, G. A. Clark, and F. E. Harris, *J. Chem. Phys.* **45**, 4743 (1966).
- ⁶¹D. D. Koelling, A. J. Freeman, and F. M. Mueller, *Phys. Rev. B* **1**, 1318 (1970); H. Schlosser and P. M. Marcus, *Phys. Rev.* **131**, 2529 (1963); D. D. Koelling, *ibid.* **188**, 1049 (1969).
- ⁶²W. E. Rudge, *Phys. Rev.* **181**, 1020 (1969); **181**, 1024 (1969).
- ⁶³J. O. Slater and P. DeCicco, MIT Solid State and Molecular Theory Group Quarterly Progress Report No. 50, p. 46 (1963) (unpublished).
- ⁶⁴J. E. Falk and R. J. Fleming, *J. Phys. C* **6**, 2954 (1973).
- ⁶⁵R. S. Mulliken, *J. Chem. Phys.* **23**, 1833 (1955).
- ⁶⁶P. O. Löwdin, *J. Chem. Phys.* **18**, 365 (1950).
- ⁶⁷R. C. Chaney, T. K. Tung, C. C. Lin, and E. E. Lafon, *J. Chem. Phys.* **52**, 361 (1970).
- ⁶⁸Similar sharp features in the initial $\Delta\rho(\vec{r})$ have been previously observed in a non-self-consistent calculation on solid SiC (Ref. 9) and in Hartree-Fock calculations on simple diatomic molecules (Ref. 69).
- ⁶⁹R. F. W. Bader and A. D. Bandrauk, *J. Chem. Phys.* **49**, 1653 (1968).
- ⁷⁰G. W. Pratt, *Phys. Rev.* **88**, 1217 (1952).
- ⁷¹Similar effects have been previously indicated in a study of the muffin-tin superposition model in molecules (Ref. 10) in which the eigenvalues and orbitals obtained in the superposition approximation were indicated to be reasonable approximations to the "exact" results, while the binding energy in that model could differ by as much as (100–300)% relative to the "full" model including the residual charge $\Delta\rho(\vec{r})$.
- ⁷²F. Herman, *Phys. Rev.* **88**, 1210 (1952); **93**, 1214 (1954).
- ⁷³W. E. Rudge (unpublished); results of band structure

cited by J. R. Leite, B. I. Bennett, and F. Herman, Phys. Rev. B 12, 1466 (1975).

⁷⁴In the LCAO calculations of Chaney, Lin, and Lafon (Ref. 11) as well as in the LCBO study of Kelvin and Lafon (Ref. 12a), and the OPW study of Bassani and Yoshimine (Ref. 3), the potential is generated from an overlapping atomic model using the Hartree-Fock charge density calculated by A. Jucy [Proc. R. Soc. Lond. A 173, 59 (1939)] for the $1s^2 2s^2 2p^2$ ground-state configuration of the carbon atom, and the crystal exchange potential is linearized to a lattice sum of atomic charge potentials. The lattice constant is taken as 6.728 a.u. In the discrete variational study of Painter *et al.* (Ref. 8), the atomic Hartree-Fock density of Clementi was used with no linearization of the exchange potential. In this work a lattice constant of 6.7406 a.u. was used.

⁷⁵As is well known, the OPW results for the states that

contain p character (e.g., Γ_{25V} , Γ_{2c} , Γ_{15c} , $X_{4,v}$, $X_{4,c}$) are probably very poorly converged since no p states appear in the carbon core and hence at these states the OPW series reduces to a pure plane-wave series. In a recent convergence study by Euwema and Stukel (Ref. 5) it was argued that some 5000 plane waves are required for complete convergence.

⁷⁶K. Schwarz, Phys. Rev. B 5, 2466 (1972).

⁷⁷J. Thewlis and A. R. Davey, Philos. Mag. 1, 409 (1958).

⁷⁸Similar ion-pair charge-transfer set were used in early quantum-mechanical calculations on simple diatomics where the Heitler-London representation in an orthogonalized basis set was reformulated to introduce ionization in the bond, e.g., J. C. Slater, J. Chem. Phys. 19, 220 (1951). This formulation was shown to yield substantial improvement over the simple molecular-orbital model.

⁷⁹A. Zunger and A. J. Freeman (unpublished).

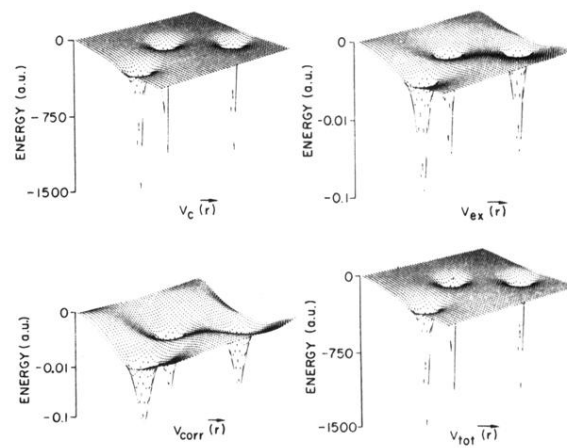


FIG. 1. Three-dimensional plots of the various components of the superposition potential in the $(1\bar{1}0)$ plane. Singular potentials are denoted by vertical dashed lines at the atomic site.

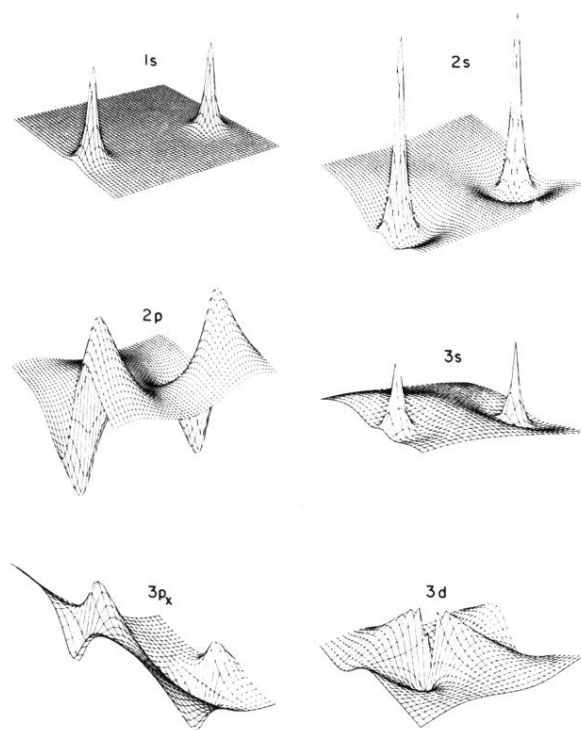


FIG. 2. Three-dimensional plots of the numerical Bloch functions at the Γ point in the BZ $(1\bar{1}0)$.

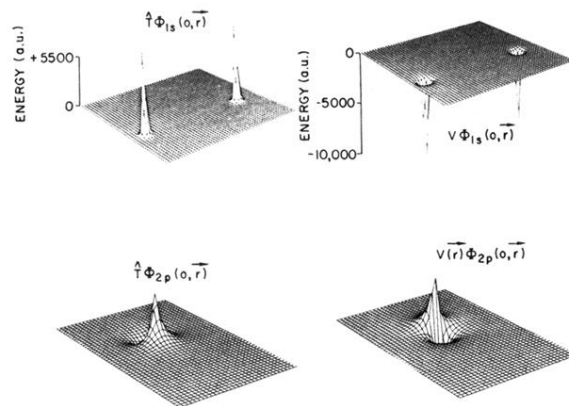


FIG. 3. Three-dimensional plots of $\hat{T}\Phi_{\mu}(0, \vec{r})$ and $V^{sp}(\vec{r})\Phi_{\mu}(0, \vec{r})$ for the Bloch states $1s$ and $2p$, in the $(1\bar{1}0)$ plane. Singular functions are denoted by the vertical dashed lines at the atomic site.